

# Adaptive covariance inflation in the ensemble Kalman filter by Gaussian scale mixtures

Patrick N. Raanes<sup>\*1</sup>, Marc Bocquet<sup>2</sup>, and Alberto Carrassi<sup>1</sup>

<sup>1</sup>Nansen Environmental and Remote Sensing Center, Thormøhlensgate 47, Bergen, N-5006, Norway

<sup>2</sup>CEREA, Joint laboratory École des Ponts ParisTech and EDF R&D, Université Paris-Est, Champs-sur-Marne, France

October 6, 2018

## Abstract

This paper studies inflation: the complementary scaling of the state covariance in the ensemble Kalman filter (EnKF). Firstly, error sources in the EnKF are catalogued and discussed in relation to inflation; nonlinearity is given particular attention. Then, the “finite-size” refinement known as the EnKF- $N$  is re-derived from a Gaussian scale mixture, again demonstrating its connection to inflation. Existing methods for adaptive inflation estimation are reviewed, and several insights are gained from a comparative analysis. One such method is selected to complement the EnKF- $N$  to make a hybrid that is suitable for contexts where model error is present and imperfectly parameterized. Benchmarks are obtained from experiments with the two-scale Lorenz model where only the slow scale is resolved. The proposed hybrid EnKF- $N$  method of adaptive inflation is found to yield systematic accuracy improvements in comparison with the existing methods, albeit to a moderate degree.

## 1 Introduction

Consider the problem of estimating the states  $\{\mathbf{x}_k \in \mathbb{R}^M\}_{k=0,1,\dots}$  given the observations  $\{\mathbf{y}_k \in \mathbb{R}^P\}_{k=1,2,\dots}$ , as generated by:

$$\mathbf{x}_k = \mathcal{M}(\mathbf{x}_{k-1}) + \boldsymbol{\xi}_k, \quad \boldsymbol{\xi}_k \sim \mathcal{N}(\mathbf{0}, \mathbf{Q}_k), \quad (1a)$$

$$\mathbf{y}_k = \mathcal{H}(\mathbf{x}_k) + \mathbf{v}_k, \quad \mathbf{v}_k \sim \mathcal{N}(\mathbf{0}, \mathbf{R}_k), \quad (1b)$$

for sequentially increasing time index  $k$ , where the noise processes,  $\{\boldsymbol{\xi}_k\}_{k \geq 1}$  and  $\{\mathbf{v}_k\}_{k \geq 1}$ , are independent in time and from each other. More specifically, the Bayesian filtering problem consists of computing and representing  $p(\mathbf{x}_k | \mathbf{y}_{k:1})$ , namely the probability density function (pdf) of the current state,  $\mathbf{x}_k$ , given all of the past observations,  $\mathbf{y}_{k:1} = \{\mathbf{y}_l\}_{l=1,\dots,k}$ . In geoscience and data assimilation (DA), the state size,  $M$ , and possibly the observation size,  $P$ , may be large (e.g.,  $10^8$ ), and  $\mathcal{M}$  and  $\mathcal{H}$  may be nonlinear [Asch *et al.*, 2016]. This necessitates approximate solution methods such as the ensemble Kalman filter (EnKF), which is simple and efficient [Evensen, 2009b].

The EnKF computes an ensemble of realizations or “members”, assumed sampled from  $p(\mathbf{x}_k | \mathbf{y}_{k:1})$ . The forecast step of the EnKF consists of the simulation of the forecast dynamics (1a) for each individual member. The analysis step considers a fixed time  $k$  only, and therefore this subscript is dropped, as is the explicit conditioning on  $\mathbf{y}_{k-1:1}$ . Thus, the forecasted prior at time  $k$  is written  $p(\mathbf{x})$ , and the analysis posterior at

time  $k$  becomes  $p(\mathbf{x} | \mathbf{y}) \propto p(\mathbf{y} | \mathbf{x}) p(\mathbf{x})$ , as given by Bayes’ rule. Denoting  $\{\mathbf{x}_n\}_{n=1,\dots,N}$  the forecasted ensemble supposedly drawn from the prior  $p(\mathbf{x})$ , the forecast sample mean and covariance are defined as:

$$\bar{\mathbf{x}} = \frac{1}{N} \sum_{n=1}^N \mathbf{x}_n, \quad (2a)$$

$$\bar{\mathbf{B}} = \frac{1}{N-1} \sum_{n=1}^N (\mathbf{x}_n - \bar{\mathbf{x}})(\mathbf{x}_n - \bar{\mathbf{x}})^\top. \quad (2b)$$

The EnKF analysis update can be derived [§6.2 of Raanes, 2016] by assuming that  $N > M$  and that  $\bar{\mathbf{x}}$  and  $\bar{\mathbf{B}}$  equal exactly the *true* moments of  $p(\mathbf{x})$ , labelled  $\mathbf{b}$  and  $\mathbf{B}$ . Following these assumptions, the derivation mirrors that of the Kalman filter, yielding the posterior (analysis) moments  $\bar{\mathbf{x}}^a$  and  $\bar{\mathbf{B}}^a$ , as well as a (deterministic, “square-root”) transformation for the ensemble so as to match these. The forecast-analysis cycle is then repeated for the next time step, and so on.

Multiplicative inflation is an auxiliary technique to adjust (typically increase) the ensemble spread and thereby covariance, initially studied by Anderson and Anderson [1999]; Hamill *et al.* [2001]; Pham *et al.* [1998]. Here, the specific variant studied is that of multiplying the prior state covariance matrix,  $\bar{\mathbf{B}}$ , by the inflation factor,  $\alpha > 0$ , ahead of the analysis:

$$\bar{\mathbf{B}} \mapsto \alpha \bar{\mathbf{B}}. \quad (3)$$

The need for inflation may arise from intrinsic deficiencies of the EnKF such as sampling error, “due to” the finite size of the ensemble, or a suboptimal treatment of non-Gaussianity. Inflation may also be necessary as a heuristic but pragmatic treatment for extrinsic deficiencies, i.e. model or observational errors.

It is difficult to formulate directives for the tuning configurations of the EnKF with any generality. Concerning inflation,  $\alpha$ , it may be that the accuracy of the EnKF is improved either by well-tuned (i.e. fixed) inflation ( $\alpha > 1$ ) or deflation ( $\alpha < 1$ ). As detailed by section 2.2, sampling error promotes the use of inflation. By contrast, the consequences of non-Gaussianity are less transparent. Nevertheless, it generally seems reasonable to inflate because non-Gaussianity is an error (intrinsic to the EnKF) *adding* to other errors. Similarly, inflating is typically required in conditions of extrinsic error such as model error [Li *et al.*, 2009; Whitaker and Hamill, 2012]. On the other hand, if the value of  $\mathbf{Q}$  being used is excessive, then deflation could be better suited. Further specificity in these guidelines is difficult to deduce. Therefore, the use of inflation traditionally requires application-specific, off-line tuning, sometimes at significant expense.

An alternative strategy that has proven successful is that of adaptive inflation, estimated on-line. The EnKF- $N$  [Bocquet *et al.*, 2015, hereafter Boc15] is a refinement of the analysis step of the EnKF that explicitly accounts for sampling error in  $\bar{\mathbf{x}}$  and  $\bar{\mathbf{B}}$ , meaning their discrepancy from the true moments  $\mathbf{b}$  and  $\mathbf{B}$ , which are seen as uncertain, hierarchical “hyperparameters”. The derivation proceeds from the rejection of the assumption that  $\bar{\mathbf{x}}$  and  $\bar{\mathbf{B}}$  are exact [Bocquet, 2011, hereafter Boc11]. Moreover, when using a completely non-informative hyperprior for  $\mathbf{b}$  and  $\mathbf{B}$ , the EnKF- $N$  has been shown to yield a “dual” form which can be straightforwardly identified as a scheme for adaptive inflation [Bocquet and Sakov, 2012]. Its implementation only requires minor add-ons to the (square-root) EnKF, with negligible computational cost. In the ideal context, where model error is absent or accurately parameterized as detailed by section 2, the EnKF- $N$  voids the need for covariance inflation, making it opportune for synthetic experiments. However, (i) wider adaption of the EnKF- $N$  has been limited by some technically challenging aspects of its derivation. Moreover, (ii) the idealism of the above assumption means that the EnKF- $N$  would still be reliant on ad-hoc inflation tuning in real-world, operational use.

This paper addresses both of the above issues of the EnKF- $N$ . Firstly, by re-deriving it with a focus on inflation, section 3 further elucidates the theory of the EnKF- $N$  and inflation. Then, section 4 reviews the literature on adaptive inflation. In contrast to the EnKF- $N$ , these adaptive inflation methods have hyperpriors that are time-dependent (as opposed to being “reset” at each analysis time) making them suitable for contexts where model error is present and imperfectly parameterized.

Section 5 uses one such method to complement the EnKF- $N$  and create a new, hybrid method. Section 6 presents benchmark experiments of the various adaptive inflation methods introduced in sections 4 and 5. Expressions and properties of the standard parametric pdfs in use in this paper,  $\mathcal{N}$ ,  $\mathcal{t}$ ,  $\chi^{+2}$ ,  $\chi^{-2}$ ,  $\mathcal{W}^{+1}$ ,  $\mathcal{W}^{-1}$ , can be found in appendix A.

## 2 Idealistic contexts and sampling error

General-purpose adaptive inflation is considered from section 4 and onward. By contrast, this section is restricted to the causes and effects of sampling error. Section 3 then shows how sampling error is partially remedied by the EnKF- $N$ .

### 2.1 Two univariate experiments

Consider the univariate (scalar) filtering problem with an initial prior  $p(x) = \mathcal{N}(x|0, 2)$ , and where the likelihood  $p(y|x) = \mathcal{N}(0|x, 2)$  and dynamical model  $\mathcal{M}_{\text{Lin}}(x) = \sqrt{2}x$  repeat identically for each time index. As is perfectly computed by the Kalman filter, the initial posterior is then  $p(x|y) = \mathcal{N}(x|0, 1)$ , yielding a forecasted prior that is identical to the initial prior. The cycle thus repeats identically through time.

Now consider the same problem except with nonlinear dynamics:  $\mathcal{M}_{\text{NonLin}}(x) = \sqrt{2}F_{\mathcal{N}}^{-1}(F_{\chi}(x^2))$ , where  $F_{\chi}$  is the cumulative distribution function (CDF) for  $\chi^{+2}(\cdot|1, 1)$ , and  $F_{\mathcal{N}}^{-1}$  is the inverse CDF for  $\mathcal{N}(\cdot|0, 1)$ . This model has the property of maintaining Gaussianity despite being nonlinear: if  $p(x|y) = \mathcal{N}(x|0, 1)$  then  $\mathcal{M}_{\text{NonLin}}(x)$  has the pdf  $\mathcal{N}(\cdot|0, 2)$ , so that the nonlinear DA problem has exactly the same solution as the linear one.<sup>1</sup>

However, as illustrated in Figure 1, applying a deterministic square-root EnKF (without any inflation or other fixes) to the two problems yields significantly contrasting results. The initial ensemble is identical for both cases, consisting of  $N = 40$  members drawn randomly from  $p(x)$ . But, in the linear case, the resulting sampling errors are quickly attenuated, and the ensemble statistics converge to the exact ones.

By contrast, in the nonlinear case, the jitteriness (sampling error) is chronic. This demonstrates that sampling error may arise purely due to nonlinearity, i.e. without actual stochasticity. Furthermore, note that the true distributions are perfectly Gaussian, and therefore the EnKF would yield the exact solution if  $N$  were infinite. Thus, even though nonlinearity typically yields non-Gaussianity, this is not always the case. Hence, the

<sup>1</sup>For context, note that  $\mathcal{M}_{\text{NonLin}}$  (i) is V-shaped, with a singularity at 0, (ii) is closely approximated as  $\mathcal{M}_{\text{NonLin}}(x) \approx \sqrt{2}\{0.88|x| + 0.23 \log(x^2) - 0.4\}$ , (iii) applied to the Gaussian, it may be visualized as folding it up in the middle, and then smearing it back out again, (iv) may be generalized to higher dimensionality by expressing  $\mathbf{x}$  in polar coordinates, since  $p(\|\mathbf{x}\|^2) = \chi^{+2}(\|\mathbf{x}\|^2|M, M)$  if  $p(\mathbf{x}) = \mathcal{N}(\mathbf{x}|\mathbf{0}, \mathbf{I}_M)$ .

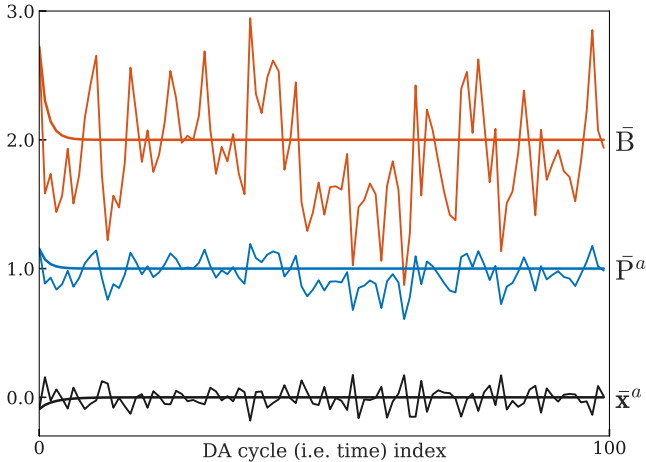


**Figure 1:** Time series of statistics from the EnKF applied to the univariate DA problem with  $\mathcal{M}_{\text{Lin}}$  (smooth lines) and  $\mathcal{M}_{\text{NonLin}}$  (jittery lines).

issue of sampling error, even if caused by nonlinear models, can be analysed and addressed separately from the issue of non-Gaussianity.

An instructive scenario of the nonlinear experiment is that in which the initial ensemble has a mean of 0 and a variance of 2, exactly. Despite the “perfect” initialization, sampling errors will still be generated. However, this error is not immediately as big as if the ensemble were actually sampled from  $x_n \sim \mathcal{N}(0, 2)$ , in which case the expected squared error of  $\bar{\mathbf{B}}$  can be shown to be  $\mathbb{E}[\bar{\mathbf{B}} - 2]^2 = 8/(N-1)$ . Indeed, repeated experiments indicate that it takes about 5 consecutive applications of  $\mathcal{M}_{\text{NonLin}}$  for the ensemble to saturate at a noise level of  $8/(N-1)$ . This gradual build-up also reflects the rule-of-thumb that stronger nonlinearity breeds larger sampling error.

## 2.2 Cataloguing the circumstances for inflation

This subsection is summarized in Table 1, whose rows correspond to specific paragraphs, as numbered.

**Table 1:** Summary of section 2.2 which discusses various filtering contexts and the consequent need for inflation. The background assumptions are idealistic:  $\mathcal{M}, \mathcal{H}, \mathbf{Q}, \mathbf{R}$  are perfectly known, and  $p(\mathbf{x})$  and  $p(\mathbf{y}|\mathbf{x})$  are always Gaussian. The star (\*) means “in either case”.

§	Ensemble size ( $N$ )	Treatment of noises ( $\mathbf{Q}, \mathbf{R}$ )	Models ( $\mathcal{M}, \mathcal{H}$ )	Should inflate?
1	$\infty$	*	*	No
2	$(M, \infty)$	Stochastic	*	Yes
3	$(M, \infty)$	*	Nonlin.	Yes
4	$(M, \infty)$	Deterministic	Linear	No
5	$[2, M]$	*	*	Yes

§1. An important property of the EnKF is that it is a consistent estimator in the linear-Gaussian case [Le Gland *et al.*, 2009; Mandel *et al.*, 2011]: at each time  $k$ , the EnKF statistics  $\bar{\mathbf{x}}$  and  $\bar{\mathbf{B}}$  converge (in probability, as  $N \rightarrow \infty$ ) to the true moments,  $\mathbf{b}$  and  $\mathbf{B}$ . Clearly, in this context, inflating or deflating will degrade the ensemble estimates.

§2. Stochastic forms of the EnKF employ pseudo-random “observation perturbations” for the analysis update step. Similarly, the forecast step may simulate additive or more advanced stochastic parameterizations of the forecast noise. With  $N < \infty$ , this introduces sampling error and thereby, as discussed further below, the need for inflation. Moreover, as shown by the theory of the EnKF- $N$  in section 3, the observations,  $\mathbf{y}$ , contain information that can improve estimates of prior hyperparameters “before” utilising  $\mathbf{y}$  to update the state vector,  $\mathbf{x}$ , thereby reducing sampling error.

§3. Deterministic, “square-root update” forms of the EnKF (which may also be formulated for the forecast noise [Raanes *et al.*, 2015]) do not introduce sampling error. Yet, with  $N < \infty$ , sampling errors arise due to model nonlinearities. This was illustrated in the experiments of Figure 1, and is further analysed in appendix B as well as in Boc15.

One cause of the typical need for  $\alpha > 1$  is that, whether due to nonlinearity or actual stochasticity, the presence of sampling error in  $\bar{\mathbf{B}}$ , computed from an ensemble drawn from  $\mathcal{N}(\mathbf{b}, \mathbf{B})$ , gives rise to the following bias [Snyder, 2012; van Leeuwen, 1999]. Even though  $\mathbb{E}[\bar{\mathbf{B}}] = \mathbf{B}$ , the posterior ensemble covariance matrix is negatively biased:

$$\mathbb{E}[\text{tr}(\bar{\mathbf{P}}^a)] < \text{tr}(\mathbf{P}^a), \quad (4)$$

where  $\mathbf{P}^a = (\mathbf{B}^{-1} + \mathbf{H}^T \mathbf{R}^{-1} \mathbf{H})^{-1}$  and  $\bar{\mathbf{P}}^a = (\bar{\mathbf{B}}^{-1} + \mathbf{H}^T \mathbf{R}^{-1} \mathbf{H})^{-1}$ , with  $\mathbf{H}$  being the presumed linear observation operator. It is the nonlinearity (concavity) of  $\bar{\mathbf{P}}^a$  as a function of the prior ensemble that causes the bias. The bias is slightly visible in the nonlinear experiment of section 2.1, where the covariances,  $\bar{\mathbf{B}}$  and  $\bar{\mathbf{P}}^a$ , are on average lower (long-run averages: 1.95 and 0.98) than the true values. Analytical, quantitative results on the bias have been obtained for the general, multivariate case by Furrer and Bengtsson [2007]; Sacher and Bartello [2008]. However, the degree of the approximation is not entirely clear, the assumption of the ensemble being truly stochastic is unreliable, and the related correctional methods were only moderately successful. An alternative approach is that of §15.3 of Evensen [2009a], where the bias is empirically estimated by using a companion ensemble of white noise. As discussed in section 3.1, a significant drawback of the inflation methods targeting this bias is that they do not establish a feedback mechanism through the cycles of DA.

There is a misconception that this bias leads to ensemble “collapse”, meaning that  $\bar{\mathbf{P}}^a \rightarrow \mathbf{0}$  and  $\bar{\mathbf{B}} \rightarrow \mathbf{0}$  as  $k \rightarrow \infty$ . But no matter how acute the single-cycle bias is, its accumulation will saturate, because it is counteracted by reductions in  $\bar{\mathbf{K}} = \bar{\mathbf{B}} \mathbf{H}^T (\mathbf{H} \bar{\mathbf{B}} \mathbf{H}^T + \mathbf{R})^{-1}$ . A related

but separate issue is “divergence”: the situation where the actual error is far larger than expected from  $\bar{\mathbf{B}}$ . If the bias is not treated by inflation or otherwise, the resulting overconfidence greatly increases the potential for divergence. In our experience, divergence is more prone to occur in the nonlinear, chaotic context, because it leads into a vicious cycle where the forecasts aggravate the situation. By contrast, the penalty for not inflating tends to be less catastrophic in the linear context, even though divergence is still possible [Fitzgerald, 1971].

§4. Furthermore, with a deterministic, square-root EnKF in the linear context, sampling error can only come from the initial ensemble and, as was observed in the experiments of section 2.1, it will be attenuated through the filtering cycles. Thus, except perhaps from an initial transitory period, it is not advisable to use inflation here. However, this conclusion is not always apparent from numerical experiments, because numerical instabilities (or its countermeasures, such as regularization) may allow for improved accuracy with some inflation.

The attenuation of sampling errors can be understood as follows. Apart from the erroneous initial covariance, the square-root EnKF is here analytically equivalent to the Kalman filter [Bocquet and Carrassi, 2017]. But then the covariance obeys the Riccati recurrence, which forgets its initial (erroneous) condition, also in the case of  $\mathbf{Q} = \mathbf{0}$  [Bocquet *et al.*, 2017]. Thus convergence holds for any  $N \geq M$ , with a rate independent of  $N$ . Interestingly, a similar analysis reveals that the choice of covariance estimate normalization (usually  $\frac{1}{N-1}$ , or  $\frac{1}{N}$ ) does not impact the EnKF mean (in the linear context): it always converges to the true mean as  $k \rightarrow \infty$ . This suggests that the success of the EnKF does not so much depend on being “unbiased” in one sense or another, but rather on this inherent stability of the filtering recurrences.

§5. The performance of the EnKF is very dependent on the ensemble size: decreasing  $N$  increases the sampling error, as well as the bias of equation (4). Furthermore, if  $N \leq M$ , then the ensemble is said to be rank-deficient; this is a separate issue from sampling error, with the grave consequence that the truth,  $\mathbf{x}$ , will not lie entirely within the ensemble subspace (c.f. section 3.5). If the distance of the truth to the ensemble subspace is moderate then localization, by virtue of operating marginally, can approximately correct for it (as well as diminish off-diagonal sampling errors, i.e. spurious correlations). Inflation does not address the rank issue directly, but will be necessary for the following reasons: (i) all of the above conditions pertaining to sampling error remain in effect; (ii) errors outside of the ensemble subspace interact with and increase the errors within [Grudzien *et al.*, 2017]; (iii) by eliminating prior correlations, localization affects an overly uncertain prior, and thus yields too strong a reduction of the ensemble spread<sup>2</sup>.

<sup>2</sup>Formally, quantify the reduction via  $|\mathbf{I}_P - \mathbf{H}\bar{\mathbf{K}}| = |\mathbf{R}|/|\mathbf{H}\bar{\mathbf{B}}\mathbf{H}^\top + \mathbf{R}|$ , the determinant of the reduction in the variance. Localization decreases the magnitude of the off-diagonals of  $\mathbf{H}\bar{\mathbf{B}}\mathbf{H}^\top + \mathbf{R}$ , provided the eigen-structures of the two terms are not too dissimilar. Thus,

Assuming  $\mathbf{Q} = 0$ , the long-run ( $k \rightarrow \infty$ ) rank of the true state covariance,  $\mathbf{B}$ , is the number of non-negative Lyapunov exponents,  $0 \leq n_0 \leq M$ , of the dynamics. This also holds approximately in the non-linear context, and means that the rank deficiency of the ensemble may be much less severe than  $M - N$  [Bocquet and Carrassi, 2017]. With this assumption, a duplicate of Table 1 applies, where  $M$  is replaced by  $n_0$ .

### 3 Re-deriving the dual EnKF- $N$ via a Gaussian scale mixture

This section gives a new derivation of the dual EnKF- $N$ . Subsection 3.1 outlines the main ideas. The details are filled in by the subsequent subsections.

#### 3.1 Overview of the derivation

Recall that the time index subscript is dropped for all objects associated with the current time ( $k$ ) such as the current “true” state  $\mathbf{x}$  and observation  $\mathbf{y}$ , but re-introduce momentarily the explicit conditioning on the past observations,  $\mathbf{y}_{k-1:1}$ . Suppose that the Bayesian forecasted prior is Gaussian, with mean  $\mathbf{b}$  and covariance  $\mathbf{B}$ :

$$p(\mathbf{x}|\mathbf{y}_{k-1:1}) = \mathcal{N}(\mathbf{x}|\mathbf{b}, \mathbf{B}). \quad (5)$$

Assume that the sample  $\mathbf{E} = [\mathbf{x}_1, \dots, \mathbf{x}_n, \dots, \mathbf{x}_N]$  is an “ensemble”, meaning that its members (i.e. the columns of  $\mathbf{E}$ ) are statistically indistinguishable from the truth [Wilks, 2011], having been iid drawn from the very same distribution (5). This assumption is convenient, but could be too idealistic in case of severe inbreeding, non-Gaussianity, and model error. Conversely, it may be too agnostic in case the ensemble is not fully random, as discussed in section 2.1.

Computational constraints induce the approximation  $p(\mathbf{x}|\mathbf{y}_{k-1:1}) \approx p(\mathbf{x}|\mathbf{E})$ , i.e. the reduction of the information of  $\mathbf{y}_{k-1:1}$  to that represented by the forecast ensemble,  $\mathbf{E}$ . Thus, while in principle (with infinite computational resources) the “true moments”,  $\mathbf{b}$  and  $\mathbf{B}$ , are known, this is not so when employing the EnKF. Here, all that is known about  $\mathbf{b}$  and  $\mathbf{B}$  comes from  $\mathbf{E}$ .

The appropriate response is to consider all of the possibilities; indeed, since by the above assumptions,  $p(\mathbf{x}, \mathbf{b}, \mathbf{B}|\mathbf{E}) = \mathcal{N}(\mathbf{x}|\mathbf{b}, \mathbf{B})p(\mathbf{b}, \mathbf{B}|\mathbf{E})$ , marginalization yields:

$$p(\mathbf{x}|\mathbf{E}) = \int_{\mathcal{B}} \int_{\mathbb{R}^M} \mathcal{N}(\mathbf{x}|\mathbf{b}, \mathbf{B}) p(\mathbf{b}, \mathbf{B}|\mathbf{E}) d\mathbf{b} d\mathbf{B}, \quad (6)$$

localization increases the denominator, hence reducing  $\mathbf{I}_P - \mathbf{H}\bar{\mathbf{K}}$  and the posterior variance.

where  $\mathcal{B}$  is the set of  $M \times M$  (symmetric) positive-definite matrices<sup>3</sup>. Equation (6) says that the “effective prior”,  $p(\mathbf{x}|\mathbf{E})$ , is a continuous mixture: the average of the “candidate priors”,  $\mathcal{N}(\mathbf{x}|\mathbf{b}, \mathbf{B})$ , as weighted by the mixing distribution,  $p(\mathbf{b}, \mathbf{B}|\mathbf{E})$ . Since the distribution of the state,  $\mathbf{x}$ , depends on the abstract parameters  $\mathbf{b}$  and  $\mathbf{B}$  that are themselves unknown, these are called hyperparameters and this layered structure is called hierarchical.

The standard EnKF is recovered from equation (6) by assuming that the sample mean and covariance,  $\bar{\mathbf{x}}$  and  $\bar{\mathbf{B}}$  of equation (2), are exact, as if  $N = \infty$ , implying a mixing distribution consisting of Dirac delta functions:  $p(\mathbf{b}, \mathbf{B}|\mathbf{E}) = \delta(\mathbf{b} - \bar{\mathbf{x}})\delta(\mathbf{B} - \bar{\mathbf{B}})$ . The EnKF- $N$  does not make this approximation, but instead acknowledges that  $N$  is finite (whence the “finite-size” moniker). The mixing distribution is obtained with Gaussian sampling theory and a non-informative hyperprior,  $p(\mathbf{b}, \mathbf{B})$ .

The connection to inflation comes from noting, as will be proven later, that equation (6) reduces to:

$$p(\mathbf{x}|\mathbf{E}) = \int_{\alpha > 0} \mathcal{N}(\mathbf{x}|\bar{\mathbf{x}}, \alpha\bar{\mathbf{B}}) p(\alpha|\mathbf{E}) d\alpha, \quad (7)$$

which is a mixture of candidate Gaussians over a scalar, scale parameter, only. For now,  $N > M$  is assumed, in which case  $\bar{\mathbf{B}}^{-1}$  exists [almost surely, as per theorem 3.1.4 of Muirhead, 1982]. The mixture (7) is illustrated by the orange elements of Figure 2. The candidate (prior) Gaussians are distinguished solely by the scaling,  $\alpha$ , of the covariance,  $\bar{\mathbf{B}}$ . Only a finite selection of the continuous family of candidate priors is plotted, the selection being representative of the mixing distribution,  $p(\alpha|\mathbf{E})$ . Interestingly, as detailed later, this yields an effective prior,  $p(\mathbf{x}|\mathbf{E})$ , which is not Gaussian, but rather a (Student’s)  $t$  distribution.

The effective posterior is given by Bayes’ rule:  $p(\mathbf{x}|\mathbf{E}, \mathbf{y}) \propto p(\mathbf{y}|\mathbf{x})p(\mathbf{x}|\mathbf{E})$ , i.e. the pointwise multiplication of the effective prior and the (Gaussian) likelihood; it is neither Gaussian nor a  $t$  distribution, and its expression does not appear to have a convenient reduction. This poses a computational challenge in high-dimensional problems, and the question of how the posterior (or an ensemble thereof) is to be computed in practice. Progress can be made by noting that the averaging over the prior moments can be “delayed” until after application of Bayes’ rule, i.e.

$$p(\mathbf{x}|\mathbf{E}, \mathbf{y}) \propto \int \underbrace{\mathcal{N}(\mathbf{y}|\mathbf{H}\mathbf{x}, \mathbf{R}) \mathcal{N}(\mathbf{x}|\bar{\mathbf{x}}, \alpha\bar{\mathbf{B}})}_{p(\mathbf{x}, \mathbf{y}|\alpha, \mathbf{E})} p(\alpha|\mathbf{E}) d\alpha. \quad (8)$$

Thus, the effective posterior can also be seen as the average of the (Gaussian) candidate posteriors,  $p(\mathbf{x}|\alpha, \mathbf{y}, \mathbf{E})$ , each of which is given by the Kalman filter formulae for a given  $\alpha$ , which can be computed very efficiently for a range of values of  $\alpha$ .

The by-product of Bayes’ rule is the “evidence”,  $p(\mathbf{y}|\alpha, \mathbf{E})$ . In this context, it is not a constant, but instead constitutes the likelihood of the mixing parameter,  $\alpha$ . Therefore, unlike all of the other curves in Figure 2, the candidate posteriors have not been normalized to integrate to 1, but instead  $p(\mathbf{y}|\alpha, \mathbf{E}) \times c$ .

The constant  $c$  been inserted and set such that the particular candidate posterior whose mode coincides with that of the effective posterior also shares its height. This makes it visible that no candidate posterior is fully coincident with the effective posterior. Nevertheless, it seems a reasonable *approximation*. But this candidate posterior corresponds to a candidate prior, which merely amounts to choosing a particular prior inflation,  $\alpha_*$ . The approximation can thus be written as:

$$p(\mathbf{x}|\mathbf{E}, \mathbf{y}) \approx p(\mathbf{x}|\alpha_*, \mathbf{E}, \mathbf{y}), \quad (9)$$

meaning that the integral over the hyperparameter,  $\alpha$ , for the effective posterior (8), is replaced by using a particular value,  $\alpha_*$ , which is chosen after taking into account  $\mathbf{y}$ . This approximation is a form of “empirical Bayes”, known as such because the prior is approximated in a way that depends on the observations,  $\mathbf{y}$ . This may appear to over-use the observations,  $\mathbf{y}$ , but it is merely an artefact of the approximation. It can be further comprehended by decomposing the integrand of equation (8) as the two factors:  $p(\mathbf{x}, \alpha|\mathbf{E}, \mathbf{y}) = p(\mathbf{x}|\alpha, \mathbf{E}, \mathbf{y}) p(\alpha|\mathbf{E}, \mathbf{y})$ , making it clear that the observations should condition *both* the state and the hyperparameter.

A posterior ensemble corresponding to the approximate posterior (9) may be computed using standard EnKF formulae, except with  $\bar{\mathbf{B}}$  replaced by the selected value,  $\alpha_*\bar{\mathbf{B}}$ . Provided that the choice among the approximating Gaussian posteriors is judicious, it stands to reason that the resulting ensemble yields an improved analysis compared to that of the standard EnKF. After all, the standard EnKF chooses its covariance estimate ( $\mathbf{B} = \bar{\mathbf{B}}$ ) before taking into account  $\mathbf{y}$ . By contrast, the EnKF- $N$  only makes this choice ( $\mathbf{B} = \alpha_*\bar{\mathbf{B}}$ ) after conditioning on  $\mathbf{y}$ . For the same reason, even though the EnKF- $N$  does not target a particular form of unbiasedness, improvement could be expected compared to the methods targeting “single-cycle unbiasedness”, described below equation (4).

However, the main asset of the EnKF- $N$  is that its secondary dependence in  $\mathbf{y}$  implicitly establishes a “theoretically tuned” *negative feedback* loop via the sequential cycling of DA: if the covariance estimate was too small at time  $k$ , this will likely be “felt” and adjusted for at  $k+1$ . The main drawback of the EnKF- $N$  is that it uses a static hyperprior, so that no explicit accumulation of past information takes place for the hyperparameters, which otherwise could have been used to account for model error. Redressing this is the subject of section 4 and onwards.

<sup>3</sup> $\mathcal{B}$  is the Euclidean space  $\mathbb{R}^{M(M+1)/2}$  corresponding to the  $M(M+1)/2$  upper-triangular elements in  $\mathbf{B}$ , restricted to positive-definite matrices (the conic subset wherein  $\mathbf{B} > \mathbf{0}$ ).

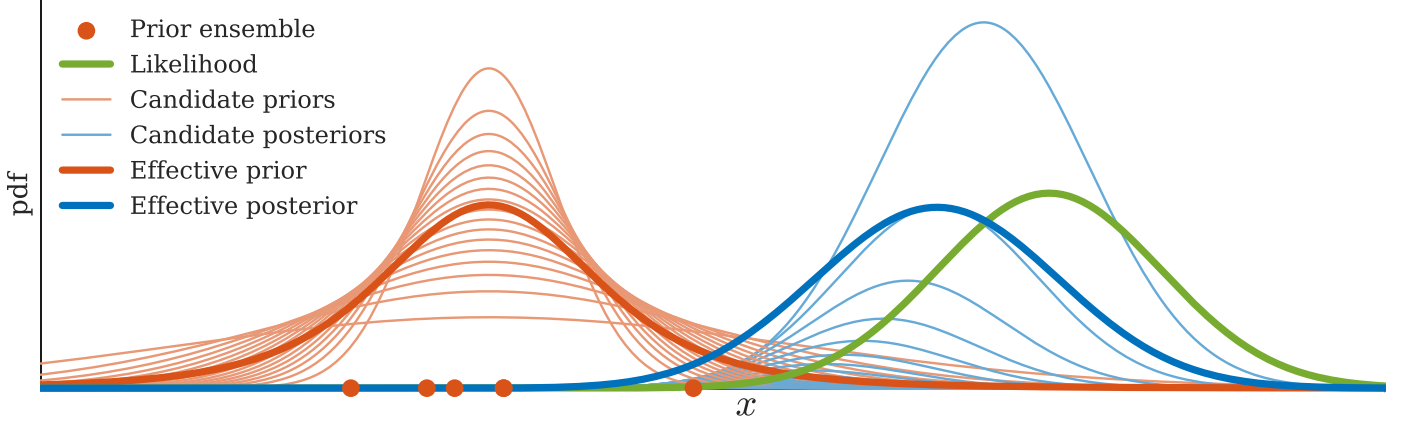


**Figure 2:** Illustration of the EnKF- $N$  as a scale mixture of Gaussians, as described in section 3.1.

### 3.2 The mixing distribution

This subsection and the next further describe equation (6) for the effective *prior*,  $p(\mathbf{x}|\mathbf{E})$ . They are largely sourced from textbooks on Gaussian sampling theory and inference, under the heading of “predictive posterior”: the probability of another draw,  $\mathbf{x}$ , from the same distribution as the sample,  $\mathbf{E}$  [e.g., §3.2 of Gelman *et al.*, 2004]. The presentation is didactic, giving meaning to intermediate stages. A concise version is provided by Boc11.

The mixing distribution in equation (6) is given by:

$$p(\mathbf{b}, \mathbf{B}|\mathbf{E}) \propto p(\mathbf{E}|\mathbf{b}, \mathbf{B}) p(\mathbf{b}, \mathbf{B}), \quad (10)$$

where  $p(\mathbf{b}, \mathbf{B})$  is a hyperprior to be specified. Here, as in Boc11, the Jeffreys priors are independently assigned to the hyperparameters:

$$p(\mathbf{b}, \mathbf{B}) = p(\mathbf{b}) p(\mathbf{B}) \propto 1 \times |\mathbf{B}|^{-(M+1)/2}. \quad (11)$$

This is a prior designed to be as non-informative (agnostic) as possible. It may be derived by positing invariance in location and scale [e.g., §12.4 of Jaynes, 2003]. By contrast, Boc15 showed the utility of using a highly informative hyperprior, suitable in contexts with little nonlinearity. Examples were also given for encoding information such as climatology or conditional statistics, resulting in a form of localization.

By the Gaussian ensemble assumption,

$$p(\mathbf{E}|\mathbf{b}, \mathbf{B}) = \prod_n \mathcal{N}(\mathbf{x}_n|\mathbf{b}, \mathbf{B}) \propto |\mathbf{B}|^{-N/2} e^{-\sum_n \|\mathbf{x}_n - \mathbf{b}\|_{\mathbf{B}}^2/2}, \quad (12)$$

where  $\|\mathbf{x}\|_{\mathbf{B}}^2 = \mathbf{x}^T \mathbf{B}^{-1} \mathbf{x}$ , which can also be written using the trace:  $\|\mathbf{x}\|_{\mathbf{B}}^2 = \text{tr}(\mathbf{x} \mathbf{x}^T \mathbf{B}^{-1})$ . Using this, and writing  $\mathbf{x}_n - \mathbf{b} = [\bar{\mathbf{x}} - \mathbf{b}] + [\mathbf{x}_n - \bar{\mathbf{x}}]$ , it can be shown that

$$\sum_n \|\mathbf{x}_n - \mathbf{b}\|_{\mathbf{B}}^2 = N \|\bar{\mathbf{x}} - \mathbf{b}\|_{\mathbf{B}}^2 + \text{tr}((N-1) \bar{\mathbf{B}} \mathbf{B}^{-1}). \quad (13)$$

Combining equations (11) to (13) for the mixing distribution (10), the resulting factors may be identified as:

$$p(\mathbf{b}, \mathbf{B}|\mathbf{E}) = \underbrace{\mathcal{N}(\mathbf{b}|\bar{\mathbf{x}}, \mathbf{B}/N)}_{p(\mathbf{b}|\mathbf{B}, \mathbf{E})} \underbrace{\mathcal{W}^{-1}(\mathbf{B}|\bar{\mathbf{B}}, N-1)}_{p(\mathbf{B}|\mathbf{E})}, \quad (14)$$

where  $\mathcal{W}^{-1}$  is the inverse-Wishart distribution (c.f. Table 2 of appendix A).

### 3.3 Integrating over the mean

Writing the integrand of equation (6) as  $p(\mathbf{x}, \mathbf{b}, \mathbf{B}|\mathbf{E}) = p(\mathbf{b}|\mathbf{x}, \mathbf{B}, \mathbf{E}) p(\mathbf{x}|\mathbf{B}, \mathbf{E}) p(\mathbf{B}|\mathbf{E})$ , the integral over  $\mathbf{b}$  becomes trivial, leaving just the latter two factors:

$$p(\mathbf{x}|\mathbf{E}) = \int p(\mathbf{x}|\mathbf{B}, \mathbf{E}) p(\mathbf{B}|\mathbf{E}) d\mathbf{B}. \quad (15)$$

Now, as may be shown by completing the square in  $\mathbf{b}$ ,

$$p(\mathbf{x}|\mathbf{b}, \mathbf{B}) p(\mathbf{b}|\mathbf{B}, \mathbf{E}) = \underbrace{\mathcal{N}(\mathbf{b}|\frac{N\bar{\mathbf{x}} + \mathbf{x}}{N+1}, \mathbf{B}/(N+1))}_{p(\mathbf{b}|\mathbf{x}, \mathbf{B}, \mathbf{E})} \underbrace{\mathcal{N}(\mathbf{x}|\bar{\mathbf{x}}, \varepsilon_N \mathbf{B})}_{p(\mathbf{x}|\mathbf{B}, \mathbf{E})}, \quad (16)$$

where  $\varepsilon_N = 1 + \frac{1}{N}$ , and the underbraces follow by identification, and provide one of the two factors in equation (15). The other,  $p(\mathbf{B}|\mathbf{E})$ , was identified in equation (14). Thus,

$$p(\mathbf{x}|\mathbf{E}) = \int \mathcal{N}(\mathbf{x}|\bar{\mathbf{x}}, \varepsilon_N \mathbf{B}) \mathcal{W}^{-1}(\mathbf{B}|\bar{\mathbf{B}}, N-1) d\mathbf{B}. \quad (17)$$

It should be appreciated that equation (17) is the same as would have resulted if  $\mathbf{b} = \bar{\mathbf{x}}$  had been assumed from the start, except for the slight adjustment of  $\varepsilon_N$  and the reduction from  $N$  to  $N-1$  in the “certainty” parameter of  $\mathcal{W}^{-1}$ . By contrast, as shown in the following, the uncertainty in  $\mathbf{B}$  has significantly more interesting consequences.

### 3.4 Reduction to a scale mixture

Define the (squared) inflation parameter:

$$s = \frac{\|\mathbf{x} - \bar{\mathbf{x}}\|_{\bar{\mathbf{B}}}^2}{\|\mathbf{x} - \bar{\mathbf{x}}\|_{\mathbf{B}}^2}. \quad (18)$$

for a given (dummy)  $\mathbf{x}$ . This section derives the scale mixture equation (7), where  $\alpha = \varepsilon_N s$ .

Given the ensemble,  $\mathbf{E}$ , the sample moments  $\bar{\mathbf{x}}$  and  $\bar{\mathbf{B}}$  are known, while  $p(\mathbf{B}|\mathbf{E}) = \mathcal{W}^{-1}(\mathbf{B}|\bar{\mathbf{B}}, N-1)$  as per equation (14). Thus, by the reciprocity of the Wishart distribution (Property 5 of appendix A),  $\mathbf{B}^{-1} \sim \mathcal{W}^{+1}(\bar{\mathbf{B}}^{-1}, N-1)$ . Property 6 can then be applied to yield  $1/s \sim \chi^{+2}(1, N-1)$ . Thus, again by reciprocity (Property 4),

$$p(s|\mathbf{E}) = \chi^{-2}(s|1, N-1), \quad (19)$$

meaning that  $s$  is inverse-chi-square (c.f. Table 2), peaking nearby 1, with certainty parameter  $N-1$ .

The derivation of equation (19) used Property 6, which is proved through characteristic functions. But the pdf  $p(s|\mathbf{E})$  can also be expressed from  $p(\mathbf{B}|\mathbf{E})$  by marginalizing over  $\mathbf{C} \in \mathcal{C}_s$ , which denotes any parameterization of the degrees of freedom in  $\mathbf{B}$  not fixed by  $s$ , i.e.  $\mathcal{C}_s = \{\mathbf{C} \in \mathbb{R}^{M(M+1)/2-1} ; \mathbf{B}(s, \mathbf{C}) \in \mathcal{B}, \|\mathbf{x} - \bar{\mathbf{x}}\|_{\mathbf{B}}^2 = \|\mathbf{x} - \bar{\mathbf{x}}\|_{s\bar{\mathbf{B}}}^2\}$ . Formally,

$$\int_{\mathcal{C}_s} p(\mathbf{B}|\mathbf{E}) J d\mathbf{C} = p(s|\mathbf{E}), \quad (20)$$

with  $J$  denoting the Jacobian determinant of  $(s, \mathbf{C}) \mapsto \mathbf{B}$ . Inserting the pdfs from equations (14) and (19):

$$\int_{\mathcal{C}_s} \mathcal{W}^{-1}(\mathbf{B}|\bar{\mathbf{B}}, N-1) J d\mathbf{C} = \chi^{-2}(s|1, N-1). \quad (21)$$

Now, rearranging the covariance mixture (17) as:

$$p(\mathbf{x}|\mathbf{E}) \propto \int_{\mathcal{B}} \exp\left(-\frac{1}{2}\|\mathbf{x} - \bar{\mathbf{x}}\|_{\varepsilon_N \mathbf{B}}^2\right) \mathcal{W}^{-1}(\mathbf{B}|\frac{N-1}{N}\bar{\mathbf{B}}, N) d\mathbf{B},$$

the same change of variables then yields:

$$p(\mathbf{x}|\mathbf{E}) \propto \int_{s>0} \exp\left(-\frac{1}{2}\|\mathbf{x} - \bar{\mathbf{x}}\|_{\varepsilon_N s \bar{\mathbf{B}}}^2\right) \left( \int_{\mathcal{C}_s} \mathcal{W}^{-1}(\mathbf{B}|\frac{N-1}{N}\bar{\mathbf{B}}, N) J d\mathbf{C} \right) ds. \quad (22)$$

The inner integral can be substituted by comparing it to equation (21), yielding:

$$\begin{aligned} p(\mathbf{x}|\mathbf{E}) &\propto \int \exp\left(-\frac{1}{2}\|\mathbf{x} - \bar{\mathbf{x}}\|_{\varepsilon_N s \bar{\mathbf{B}}}^2\right) \chi^{-2}(s|\frac{N-1}{N}, N) ds \\ &\propto \int \mathcal{N}(\|\mathbf{x} - \bar{\mathbf{x}}\|_{\bar{\mathbf{B}}} | 0, \varepsilon_N s) \chi^{-2}(s|1, N-1) ds. \end{aligned} \quad (23)$$

In conclusion, the covariance mixture of equation (17) reduces to a scale mixture. An alternative proof that does not rely on the intermediate result (19) is found in appendix C.

The scale mixture (23) has been written using the notational trick where  $\mathcal{N}$  acts as a *univariate* function; this emphasizes that  $s$  is peaked around 1 with certainty  $N-1$ . By contrast, the mixture (7) is obtained using  $\alpha = \varepsilon_N s$  and  $p(\alpha|\mathbf{E}) = \chi^{-2}(\alpha|\varepsilon_N \frac{N-1}{g}, g)$  with  $g = N - M$ .

### 3.5 Ensemble subspace parameterization

Let  $\mathbf{1}$  be the vector of ones of length  $N$ , and  $\mathbf{I}_N$  the  $N \times N$  identity matrix. Then the sample moments, given in equation (2), may be conveniently expressed as:

$$\bar{\mathbf{x}} = \mathbf{E}\mathbf{1}/N, \quad \bar{\mathbf{B}} = \frac{1}{N-1}\mathbf{A}\mathbf{A}^\top, \quad (24)$$

where  $\mathbf{A} = [\mathbf{x}_1 - \bar{\mathbf{x}}, \dots, \mathbf{x}_n - \bar{\mathbf{x}}, \dots, \mathbf{x}_N - \bar{\mathbf{x}}] = \mathbf{E}\mathbf{\Pi}_1^\perp$  is the ensemble ‘‘anomalies’’, with  $\mathbf{\Pi}_1^\perp = (\mathbf{I}_N - \mathbf{1}\mathbf{1}^\top/N)$  the orthogonal projector onto  $\text{range}(\mathbf{1})^\perp$ , the orthogonal complement space to  $\text{range}(\mathbf{1})$ .

So far it has been assumed that  $N > M$  so that  $\bar{\mathbf{B}}$  is invertible (almost surely) and that the ensemble spans the entire state space. This is unrealistic for geoscientific DA, where  $N$  rarely exceeds 100, while  $M$  may exceed  $10^9$ . More reasonably, it is henceforth assumed that the support of the forecast pdf is confined to the ensemble subspace, i.e. the affine space  $\{\mathbf{x} \in \mathbb{R}^M : [\mathbf{x} - \bar{\mathbf{x}}] \in \text{range}(\mathbf{A})\}$ . This assumption is actually conventional, as it is implicit in the standard EnKF’s assumption that  $\mathbf{b} = \bar{\mathbf{x}}$  and  $\mathbf{B} = \bar{\mathbf{B}}$  along with Gaussianity. The assumption means that the ensemble has sufficient rank. Thus one may expect tolerable accuracy of the filter, even without localization [Bocquet and Carrassi, 2017].

It is preferable to work with variables that embody the restriction of the assumption [Hunt *et al.*, 2007]; therefore, the following change of variables is done

$$\mathbf{x}(w) = \bar{\mathbf{x}} + \mathbf{A}w \quad (25)$$

where  $w \in \mathbb{R}^N$ . Note that the ensemble members expressed in the coordinate system of  $w$  are merely the coordinate vectors  $(\mathbf{x}_n = \bar{\mathbf{x}} + \mathbf{A}e_n)$ , with  $e_n$  being the  $n$ -th column of  $\mathbf{I}_N$ . Hence, in this coordinate system, the sample mean is  $\mathbf{1}/N$ , or equivalently zero, since  $\mathbf{A}\mathbf{1} = \mathbf{0}$ , and the sample covariance matrix is  $\frac{1}{N-1}\mathbf{I}_N$ . Substituting these for  $\bar{\mathbf{x}}$  and  $\bar{\mathbf{B}}$  in equation (23) is a shortcut to obtain

the effective prior for  $\mathbf{w}$ :

$$p(\mathbf{w}|\mathbf{E}) \propto \int s^{-g/2} \mathcal{N}(\|\mathbf{w}\|_{\frac{1}{N-1}\mathbf{I}_N} | 0, \varepsilon_N s) \chi^{-2}(s|1, N-1) ds, \quad (26)$$

where the presence of  $g$  is explained in the following.

Denote  $g$  the dimensionality of the nullspace of  $\mathbf{A}$ . Due to  $\mathbf{\Pi}_1^\perp$  it holds that  $g = \max(1, N-M)$ , almost surely. Thus, typically  $g = 1$ , and the parameterization in  $\mathbf{w}$  has one direction of redundancy, warranting careful attention. The issue is analogous to expressing 1 random variable as the sum of 2, or indeed expressing  $N - g$  random variables as a linear combination of  $N$ . The principle is that regardless of how the probability space is augmented with the redundant degrees of freedom, once these are marginalized out, one should be left with the original distribution. Boc15 showed that the adjustments of  $g$  in equation (26) are then required.

### 3.6 An exact approximation

Writing out the parametric pdfs of the scale mixture (26) yields:

$$p(\mathbf{w}|\mathbf{E}) = c_1 \int s^{-(N+g)/2-1} e^{-\frac{N-1}{2\varepsilon_N}(\|\mathbf{w}\|^2 + \varepsilon_N)/s} ds. \quad (27)$$

The change of variables  $s = (\|\mathbf{w}\|^2 + \varepsilon_N)/u$  factors the dependency in  $\mathbf{w}$  out of the integral and yields:

$$p(\mathbf{w}|\mathbf{E}) \propto (\varepsilon_N + \|\mathbf{w}\|^2)^{-(N+g)/2}, \quad (28)$$

which can be recognized as a  $t$  distribution with certainty parameter  $g$  (c.f. appendix A). The  $t$  distribution is elliptical and thus similar-looking to the Gaussian one [Muirhead, 1982, §1.5]; in case  $g = 1$ , it is also known as a Cauchy distribution; it has the hallmark of thick tails, which it inherits from the inverse-chi-square distribution, and which makes it suited for robust inference [Fernandez and Steel, 1999; Gelman *et al.*, 2004; Geweke, 1993; Roth *et al.*, 2017].

Unlike Boc11, here the expression (28) for the effective prior will not be used directly. Instead, with the change of variables  $s = \frac{N-1}{\varepsilon_N}/\tilde{\zeta}$ , the scale mixture (27) is rewritten:

$$p(\mathbf{w}|\mathbf{E}) = c_1 \int e^{-\frac{1}{2}\tilde{L}(\tilde{\zeta}, \mathbf{w})} d\tilde{\zeta}, \quad (29a)$$

$$\tilde{L}(\tilde{\zeta}, \mathbf{w}) = \tilde{\zeta}(\varepsilon_N + \|\mathbf{w}\|^2) - (N+g-2) \log \tilde{\zeta}. \quad (29b)$$

The second derivative is here fairly simple,  $\tilde{L}'' = \frac{\partial^2 \tilde{L}}{\partial \tilde{\zeta}^2} \propto \tilde{\zeta}^{-2}$ , making the integral (29a) suited to Laplace's approximation:

$$p(\mathbf{w}|\mathbf{E}) \approx c_1 (2\pi/\tilde{L}'')^{1/2} e^{-\frac{1}{2}\tilde{L}} \Big|_{(\tilde{\zeta}(\mathbf{w}), \mathbf{w})}, \quad (30)$$

where  $\tilde{\zeta}(\mathbf{w}) = \operatorname{argmin}_{\tilde{\zeta}} \tilde{L}(\tilde{\zeta}, \mathbf{w}) = \frac{N+g-2}{\varepsilon_N + \|\mathbf{w}\|^2}$ . This form of  $p(\mathbf{w}|\mathbf{E})$  is known in statistics as a saddlepoint

approximation. But writing out  $\tilde{\zeta}(\mathbf{w})$  in equation (30) immediately yields (28), meaning that the approximation is *exact*. This is a remarkable feature known to arise in a few cases [Azevedo-Filho and Shachter, 1994; Goutis and Casella, 1999]. Again, however, the explicit substitution is avoided in favour of keeping  $\tilde{\zeta}(\mathbf{w})$  in place.

Defining  $L = \tilde{L} + \log \tilde{L}''$  simplifies equation (30) by hiding  $(\tilde{L}'')^{1/2}$  in the exponential. Moreover, it can be checked that the numerator of  $\tilde{\zeta}(\mathbf{w})$  does not impact equation (30) except through the constant  $c_1$ . This is used to rewrite the effective prior as:

$$p(\mathbf{w}|\mathbf{E}) = c_2 e^{-\frac{1}{2}L(\zeta(\mathbf{w}), \mathbf{w})}, \quad (31a)$$

$$L(\zeta, \mathbf{w}) = \zeta(\varepsilon_N + \|\mathbf{w}\|^2) - (N+g) \log \zeta, \quad (31b)$$

$$\zeta(\mathbf{w}) = \frac{N+g}{\varepsilon_N + \|\mathbf{w}\|^2}, \quad (31c)$$

with the advantage that  $\frac{\partial L}{\partial \zeta}(\zeta(\mathbf{w}), \mathbf{w}) = 0$  for any  $\mathbf{w}$ . Conversely, this means that  $\zeta$  may be treated as a free variable to be optimized for, because equation (31c) is satisfied wherever  $\frac{\partial L}{\partial \zeta} = 0$ . This tactic becomes useful and is formally exploited in the following section.

### 3.7 The posterior and its mode

Denote  $\mathcal{H}(\mathbf{E})$  the observation operator applied (column-wise) member-wise to the ensemble,  $\mathcal{H}(\mathbf{E})\mathbf{1}/N$  the sample mean of the observed ensemble,  $\mathbf{Y} = \mathcal{H}(\mathbf{E})\mathbf{\Pi}_1^\perp$  the corresponding observation anomalies, and let  $\bar{\delta} = \mathbf{y} - \mathcal{H}(\mathbf{E})\mathbf{1}/N$  be the average innovation. In the following it is assumed that the observation operator is linear,  $\mathcal{H} : \mathbf{x} \mapsto \mathbf{H}\mathbf{x}$ , so that the linear approximation  $\mathbf{y} - \mathcal{H}(\mathbf{x}(\mathbf{w})) \approx \bar{\delta} - \mathbf{Y}\mathbf{w}$  is exact. The likelihood in  $\mathbf{w}$  thus becomes  $p(\mathbf{y}|\mathbf{w}) = \mathcal{N}(\bar{\delta}|\mathbf{Y}\mathbf{w}, \mathbf{R})$ .

Define  $J = -2 \log p(\mathbf{w}|\mathbf{E}, \mathbf{y})$  plus a constant. By Bayes' rule, this log posterior reads:

$$J(\zeta, \mathbf{w}) = L(\zeta, \mathbf{w}) - 2 \log \mathcal{N}(\bar{\delta}|\mathbf{Y}\mathbf{w}, \mathbf{R}) + c \quad (32a)$$

$$= \varepsilon_N \zeta - (N+g) \log \zeta + \zeta \|\mathbf{w}\|^2 + \|\bar{\delta} - \mathbf{Y}\mathbf{w}\|_{\mathbf{R}}^2, \quad (32b)$$

where the (effective) prior has been written using  $\zeta$  as in equation (31a). Completing the square in  $\mathbf{w}$  yields:

$$J(\zeta, \mathbf{w}) = \|\mathbf{w} - \bar{\mathbf{w}}^a(\zeta)\|_{\bar{\mathbf{G}}^a(\zeta)}^2 + D(\zeta), \quad (33)$$

where the quadratic form is specified by the standard EnKF subspace analysis formulae:

$$\bar{\mathbf{G}}^a(\zeta) = (\zeta \mathbf{I}_N + \mathbf{Y}^\top \mathbf{R}^{-1} \mathbf{Y})^{-1}, \quad (34a)$$

$$\bar{\mathbf{w}}^a(\zeta) = \bar{\mathbf{G}}^a(\zeta) \mathbf{Y}^\top \mathbf{R}^{-1} \bar{\delta}, \quad (34b)$$

and  $D$  should be recognized as “dual”, as in Bocquet and Sakov [2012]:

$$D(\zeta) = \varepsilon_N \zeta - (N+g) \log \zeta + \|\bar{\delta}\|_{\mathbf{R} + \mathbf{Y}\mathbf{Y}^\top/\zeta}^2. \quad (35)$$

Now,  $\zeta$  depends on  $\mathbf{w}$ , and so the maximization of  $p(\mathbf{w}|\mathbf{E}, \mathbf{y})$  is not as obvious as equation (33) suggests.



Fortunately, to find a critical point, it suffices to satisfy

$$\frac{\partial J}{\partial \mathbf{w}} = \mathbf{0}, \quad (36a)$$

$$\frac{\partial J}{\partial \zeta} = 0. \quad (36b)$$

This is because the criteria (36a) and (36b) imply  $\frac{dJ}{d\mathbf{w}} = \frac{\partial J}{\partial \mathbf{w}} + \frac{\partial J}{\partial \zeta} \frac{d\zeta}{d\mathbf{w}} = \mathbf{0}$ , where  $\zeta(\mathbf{w})$  is given by equation (31c), which is enforced since  $\frac{\partial L}{\partial \zeta} = 0$ , as follows from equations (32a) and (36b).

Now, the first criterion (36a) is trivially satisfied by setting  $\mathbf{w} = \bar{\mathbf{w}}^a(\zeta)$  for a given  $\zeta$ , as seen from equation (33). But it can also be seen that  $J = D$  along the constraint  $\mathbf{w} = \bar{\mathbf{w}}^a(\zeta)$ , and so

$$\frac{dD}{d\zeta} = \frac{dJ}{d\zeta} = \frac{\partial J}{\partial \zeta} + \frac{\partial J}{\partial \mathbf{w}} \frac{d\mathbf{w}}{d\zeta} = \frac{\partial J}{\partial \zeta}. \quad (37)$$

Hence  $\frac{dD}{d\zeta} = 0$  implies the second criterion (36b).

In conclusion,  $\mathbf{w} = \bar{\mathbf{w}}^a(\zeta_*)$  is a critical point of the effective posterior if and only if  $\zeta_*$  is a local minimizer of  $D(\zeta)$ . Since both of the terms  $D(\zeta)$  and  $\|\mathbf{w} - \bar{\mathbf{w}}^a\|_{\bar{\mathbf{G}}^a}^2$  of equation (33) are here individually minimized, this critical point must be a minimum, as was found by duality theory by Bocquet and Sakov [2012]. Hence the high-dimensional, non-Gaussian mode-finding problem for  $p(\mathbf{w}|\mathbf{E}, \mathbf{y})$  may be exchanged for a scalar optimization problem.

The optimization of  $D(\zeta)$  requires iterating, but each evaluation is computationally trivial, provided the singular value decomposition (SVD),

$$\mathbf{U} \text{diag}(\sigma_1, \dots, \sigma_P) \mathbf{V}^\top = [(N-1)\mathbf{R}]^{-1/2} \mathbf{Y}, \quad (38)$$

has been obtained beforehand, as is typical to compute equation (34). Multiple minima are a rarity; in such cases  $\zeta_*$  will depend on the optimizer and initial guess, here Newton’s method and  $\zeta = N - 1$ .

To obtain an analysis posterior *ensemble*, a Gaussian approximation to the distribution is chosen. In addition to its simplicity, twin experiments [Boc11; Boc15; Boc12] have provided solid support to using:

$$p(\mathbf{w}|\mathbf{E}, \mathbf{y}) \approx \mathcal{N}(\mathbf{w}|\bar{\mathbf{w}}^a(\zeta_*), \bar{\mathbf{G}}^a(\zeta_*)). \quad (39)$$

Notably, this approximation matches the mode and Hessian of the exact  $p(\mathbf{w}|\mathbf{E}, \mathbf{y})$ . The corresponding ensemble is constructed as:

$$\mathbf{E}^a = [\bar{\mathbf{x}} + \mathbf{A}\bar{\mathbf{w}}^a(\zeta_*)] \mathbf{1}^\top + \sqrt{N-1} \mathbf{A}(\bar{\mathbf{G}}^a(\zeta_*))^{1/2}, \quad (40)$$

potentially also appending some mean-preserving orthogonal matrix to the anomalies. Note that this is “just” the symmetric square-root EnKF [i.e. the ensemble transform Kalman filter (ETKF) of Bishop *et al.*, 2001; Hunt *et al.*, 2004], except for a prior inflation of  $\alpha_* = (N-1)/\zeta_*$ .

As discussed by Boc15, the choice of candidate posterior is not unassailable, and certain modifications of the dual function can be argued on the grounds

of modifying this choice. Indeed, if the influence of the likelihood is small, as quantified by  $\bar{\sigma}^2 := \text{tr}(\mathbf{H}\mathbf{B}\mathbf{H}^\top \mathbf{R}^{-1})/P \rightarrow 0$ , then it becomes necessary to adjust the choice towards 1. Moreover, weakly linear contexts create relatively little sampling error. In such cases, the hyperprior may be too agnostic. It can be corrected for by increasing (tuning) the certainty of  $\chi^{-2}$  to a higher value than  $N-1$ , yielding a Dirac-delta in the limit. Finally, the Hessian should be corrected by subtracting  $\frac{2\zeta_*^2}{N+g} \bar{\mathbf{w}}^a \bar{\mathbf{w}}^{a\top}$ , because  $\zeta$  is not a constant [Boc15]. However, this is typically negligible and also adds a computational load, while Gaussianity remains an approximation. None of these adjustments were deemed necessary to use in the numerical experiments of this paper.

## 4 Review on adaptive inflation

The filtering problem as formulated with equations (1a) and (1b) uses additive noise processes  $\{\boldsymbol{\xi}_k\}_{k \geq 1}$  and  $\{\mathbf{v}_k\}_{k \geq 1}$  to represent model and observation errors. “Primary” filters [Dee *et al.*, 1985] assume the noise/error covariances,  $\mathbf{Q}$  and  $\mathbf{R}$ , are perfectly known. In reality, these system statistics are rarely well known; this deteriorates the state estimates and can cause filter divergence. Self-diagnosing and correcting filters which estimate and modify the given noise statistics are called “adaptive”. Adaptive Kalman filter literature include Mehra [1972]; Mohamed and Schwarz [1999]. Adaptive particle filter literature include Özkan *et al.* [2013]; Storvik [2002].

The rest of this section is concerned with adaptive filtering for DA, focusing on the EnKF and the on-line<sup>4</sup>estimation of the model error, i.e.  $\mathbf{Q}$ . Among the literature using full [Miyoshi *et al.*, 2013; Nakabayashi and Ueno, 2017] and/or diagonal [Dreano *et al.*, 2017; Ueno and Nakamura, 2016] covariance parameterizations, some success has been noted. However, the scope of this paper is restricted to the estimation of a single multiplicative inflation factor,  $\beta$ , for  $\bar{\mathbf{B}}$ . This assigns a structure to the covariance and reduces the dimensionality and complexity of the problem and thus regularizes it. The tradeoff is a bias, but this drawback is largely offset by spatialization.

Since this section reviews general-purpose adaptive inflation, the inflation factor is here labelled  $\beta$ . This contrasts it to  $\alpha$  of the EnKF- $N$ , which only targets sampling error. For brevity, the explicit conditioning on the ensemble,  $\mathbf{E}$ , is henceforth dropped. For familiarity and comparisons to literature, the distributions are written in terms of the original state variable  $\mathbf{x}$ , rather than  $\mathbf{w}$  of equation (25).

The review and following analyses serve to choose a method with which to make a hybrid EnKF- $N$

<sup>4</sup>“On-line” (or “live”) means that the estimation is included in the DA cycling loop, so as to be updated each time new data  $\mathbf{y}$  is received. Some off-line approaches not further reviewed include Dee and Da Silva [1999]; Dreano *et al.* [2017]; Mitchell and Carrasi [2015]; Ueno *et al.* [2010].

that works well with model error. The review is split between methods that may be termed “marginal”, working with  $\beta$  separately from  $\mathbf{x}$ , and “joint”, working with  $(\beta, \mathbf{x})$  simultaneously. The joint methods, including “variational Bayes” and the “hierarchical EnKF”, are theoretically appealing. However, on closer inspection, including numerical testing, they were found to be less advantageous. Therefore, the marginal methods take centre stage, while the review of the joint methods has been placed in appendix D.

#### 4.1 Marginal inflation estimation

Recall the average innovation,  $\bar{\boldsymbol{\delta}} = \mathbf{y} - \mathbf{H}\bar{\mathbf{x}}$ , where the prior ensemble mean,  $\bar{\mathbf{x}}$ , should not be confused with the true mean,  $\mathbf{b}$ , and where  $p(\mathbf{y}|\mathbf{x}) = \mathcal{N}(\mathbf{y}|\mathbf{H}\mathbf{x}, \mathbf{R})$ . Writing  $\bar{\boldsymbol{\delta}} = (\mathbf{y} - \mathbf{H}\mathbf{x}) + \mathbf{H}(\mathbf{x} - \mathbf{b}) + \mathbf{H}(\mathbf{b} - \bar{\mathbf{x}})$  it can be seen that

$$\mathbb{E}[\bar{\boldsymbol{\delta}}\bar{\boldsymbol{\delta}}^\top|\mathbf{B}] = \mathbf{R} + \mathbf{H}\varepsilon_N\mathbf{B}\mathbf{H}^\top. \quad (41)$$

A departure from non-ensemble works [e.g., Daley, 1992] is the adjustment  $\varepsilon_N = 1 + 1/N$ , which is the result of having to use  $\bar{\mathbf{x}}$  rather than  $\mathbf{b}$  to define  $\bar{\boldsymbol{\delta}}$ . However,  $\varepsilon_N$  is not typically used in the inflation literature, and is therefore ignored in the following survey.

Assuming  $\mathbf{B} = \beta\bar{\mathbf{B}}$ , the objective is to find the scaling,  $\beta$ . Making this substitution and replacing the expectation  $\mathbb{E}[\bar{\boldsymbol{\delta}}\bar{\boldsymbol{\delta}}^\top|\mathbf{B}]$  by the observed value  $\bar{\boldsymbol{\delta}}\bar{\boldsymbol{\delta}}^\top$  yields:

$$\bar{\boldsymbol{\delta}}\bar{\boldsymbol{\delta}}^\top \approx \beta\mathbf{H}\bar{\mathbf{B}}\mathbf{H}^\top + \mathbf{R} =: \bar{\mathbf{C}}(\beta), \quad (42)$$

which suggests matching (some univariate summary statistic of)  $\bar{\boldsymbol{\delta}}\bar{\boldsymbol{\delta}}^\top$  by adjusting the inflation,  $\beta$ . For example, Li *et al.* [2009] working in the framework of the ETKF, use the estimator:

$$\hat{\beta}_{\mathbf{I}} := \frac{\|\bar{\boldsymbol{\delta}}\|^2 - \text{tr}(\mathbf{R})}{\text{tr}(\mathbf{H}\bar{\mathbf{B}}\mathbf{H}^\top)}, \quad (43)$$

which follows directly from the trace of equation (42). Alternatively, the estimator of Wang and Bishop [2003] can be obtained by transforming equation (42) by  $\mathbf{R}^{-1}$  before taking the trace, thus allowing for heterogeneous observations and different units:

$$\hat{\beta}_{\mathbf{R}} := \frac{\|\bar{\boldsymbol{\delta}}\|_{\mathbf{R}}^2/P - 1}{\bar{\sigma}^2}, \quad (44)$$

where the identity  $\text{tr}(\bar{\boldsymbol{\delta}}\bar{\boldsymbol{\delta}}^\top\mathbf{R}^{-1}) = \|\bar{\boldsymbol{\delta}}\|_{\mathbf{R}}^2$  has been used, and

$$\bar{\sigma}^2 = \text{tr}(\mathbf{H}\bar{\mathbf{B}}\mathbf{H}^\top\mathbf{R}^{-1})/P. \quad (45)$$

Miyoshi [2011] proposes a variant using the Schur product  $\circ\mathbf{R}^{-1}$ . However, the regular algebra behind  $\hat{\beta}_{\mathbf{R}}$  is preferable, as it decorrelates the diagonals of  $\bar{\boldsymbol{\delta}}\bar{\boldsymbol{\delta}}^\top$  and hence diminishes the variance of their trace. Other variations are studied in appendix E.1, but are found to have more bias than  $\hat{\beta}_{\mathbf{R}}$  because of further exposure to the uncertainty in  $\bar{\mathbf{B}}$ .

It is instructive to relate equation (42) to maximum likelihood (ML) results. Assuming Gaussianity,

$$p(\mathbf{x}|\beta) = \mathcal{N}(\mathbf{x}|\bar{\mathbf{x}}, \beta\bar{\mathbf{B}}), \quad (46)$$

it can be shown that the likelihood for  $\beta$  is:

$$p(\mathbf{y}|\beta) = \mathcal{N}(\bar{\boldsymbol{\delta}}|\mathbf{0}, \bar{\mathbf{C}}(\beta)). \quad (47)$$

As is well known, the sampling law  $\boldsymbol{\delta}_k \sim \mathcal{N}(\mathbf{0}, \mathbf{C})$  yields  $K^{-1}\sum_{k=1}^K\boldsymbol{\delta}_k\boldsymbol{\delta}_k^\top$  as the ML estimate of  $\mathbf{C}$ . Thus, equation (42) can be seen as a singleton formulation of this. However, the ML estimate for  $\mathbf{C}$  is not defined unless  $K$  is larger than the number of observations,  $P$ , so the analogy is tenuous. Still, Dee [1995] noted that if  $\mathbf{C}$  is restricted to a scaling:  $\mathbf{C}(\theta) = \theta\mathbf{C}_0$  for some  $\mathbf{C}_0$ , then the ML estimate of  $\theta$  is defined:  $\|\bar{\boldsymbol{\delta}}\|_{\mathbf{C}_0}^2/P$ . But, with the parameterization  $\bar{\mathbf{C}}(\beta)$  of equation (47), the ML estimate,  $\hat{\beta}_{\text{ML}}$ , is not analytically available, and will require iterations [e.g., Liang *et al.*, 2012; Mitchell and Houtekamer, 2000; Zheng, 2009].

The accumulation and memorization of past information has gradually become more sophisticated. Wang and Bishop [2003] take the geometric average of  $\hat{\beta}_{\mathbf{R}}$  over time, while Mitchell and Houtekamer [2000] use the median of instantaneous ML estimates. Lacking the fuller Bayesian setting, neither yields consistency (convergence to the true value) in time, because a temporal average of some point estimate  $\hat{\beta}_k$  based on  $p(\mathbf{y}_k|\beta)$  is generally not the value to which  $\beta|\mathbf{y}_{K:1}$  converges as  $K \rightarrow \infty$ . Nevertheless, this mismatch is not likely to be severe, and the simplicity of the approach is an advantage.

The approach of temporally averaging likelihood estimates has since been replaced by the more rigorous approach of filtering. It should be noted that this “secondary” filter is valid because the innovations are supposedly independent in time [Mehra, 1972]. Li *et al.* [2009] and Miyoshi [2011] assign a Gaussian prior  $p(\beta) = \mathcal{N}(\beta|\beta^f, V^f)$ , where the mean  $\beta^f$  is a persistence or relaxation of the previous analysis mean, and where the variance  $V^f$  is to be tuned. The likelihood is also assumed Gaussian:  $p(\mathbf{y}|\beta) = \mathcal{N}(\hat{\beta}|\beta, \hat{V})$ , where  $\hat{\beta} = \hat{\beta}_{\mathbf{I}}$  in Li *et al.* [2009] and  $\hat{\beta} = \hat{\beta}_{\mathbf{R}}$  in Miyoshi [2011]. In the former,  $\hat{V}$  is a tuning parameter, while the latter suggests using the variance of  $\hat{\beta}_{\mathbf{R}}$  of equation (44):

$$\hat{V} = \left[ \frac{\text{tr}(\mathbf{H}\bar{\mathbf{B}}\mathbf{H}^\top\mathbf{R}^{-1})/P + 1}{\bar{\sigma}^2\sqrt{P/2}} \right]^2 \approx \left[ \frac{\beta^f\bar{\sigma}^2 + 1}{\bar{\sigma}^2\sqrt{P/2}} \right]^2, \quad (48)$$

where the approximation comes from using  $\mathbf{B} \approx \beta^f\bar{\mathbf{B}}$ . Importantly, equation (48) has the logical consequence that the observations are given no weight when  $\bar{\sigma}^2 \rightarrow 0$  or  $P \rightarrow 0$ . The method is spatialized by associating each local analysis domain with its own inflation parameter. Localization tapering promotes smoothness of the inflation field.

Also working in the framework of a square-root EnKF, Brankart *et al.* [2010] use diffusive forecasts for

the inflation distribution. They do not sequentially approximate the posteriors, instead expressing them explicitly in terms of all of the past innovations, progressively diffused by a “forgetting exponent”,  $\phi < 1$ :

$$p(\beta|\mathbf{y}_{K:1}) \propto (p(\beta))^{\phi^K} \prod_{k=1}^K \mathcal{N}(\bar{\delta}_k|\mathbf{0}, \phi^{k-K}\bar{\mathbf{C}}_k(\beta)). \quad (49)$$

The chosen estimate,  $\hat{\beta}_{\text{MAP}}$ , is found iteratively. The requisite evaluations of the cost function is not prohibitive because the square-root formulation means that diagonalizing matrix decompositions have already been computed.

Anderson [2007], working in the framework of the EAKF, explicitly considers forecasting the (parameters of the) inflation distribution, but only tests persistence forecasts, i.e.  $p(\beta_k|\beta_{k-1}) = \delta(\beta_k - \beta_{k-1})$ . The posteriors (and hence the forecasted priors) are approximated by Gaussians: for a given time,

$$p(\beta|y_i) \approx \mathcal{N}(\beta|\hat{\beta}_{\text{MAP}}, V^a), \quad (50)$$

which are computed serially for each component  $y_i$  of the observation  $\mathbf{y}$ . The single-observation likelihood allows the maximum a posteriori (MAP) estimate  $\hat{\beta}_{\text{MAP}}$  to be found exactly and without iterations, via a cubic polynomial;  $V^a$  is fitted by requiring that equation (50) be exact for another particular value of  $\beta$ , as normalized by its value at  $\hat{\beta}_{\text{MAP}}$ . Anderson [2009] spatializes the method, associating each state variable with its own inflation parameter. Here, correlation coefficients complicate the likelihood, so that  $\hat{\beta}_{\text{MAP}}$  must be found via a Taylor expansion of the likelihood and a resulting quadratic polynomial.

Anderson [2009] also notes that a Gaussian prior does not constrain the inflation estimates to positive values. Thus, nonsensical negative estimates will occur for small innovations. Imposing some lower cap (bound), e.g.,  $\hat{\beta}_{\text{MAP}} > 0$  or even  $\hat{\beta}_{\text{MAP}} > 1$ , is done as a quick-fix. As Stroud *et al.* [2016] note, such capping causes a bias. However, this bias should be avoided by employing the un-capped values in the averaging.

Instead of ad-hoc mechanisms, using a better suited prior will make the problem disappear. Brankart *et al.* [2010] use an exponential pdf for the initial prior, but acknowledge that it is not appropriate for small  $\beta$ . Indeed, a better choice is the inverse-chi-square distribution,  $\chi^{-2}$ , also called Inverse-Gamma; it is the conjugate prior to the variance parameter of a Gaussian sample, and was shown in section 3 to be intimately linked to inflation. It has been employed in adaptive filtering by e.g., Mehra [1972]; Storvik [2002], and in an EnKF contexts by Stroud and Bengtsson [2007] and Gharamti [2017], who used it to enhance the scheme of Anderson [2009]. Similarly, the following subsection formulates the inflation filter using  $\hat{\beta}_{\mathbf{R}}$  in terms of  $\chi^{-2}$  distributions.

## 4.2 Renouncing the Gaussian framework

This subsection improves the formulation of the estimator  $\hat{\beta}_{\mathbf{R}}$ ; in particular, it abstains from assuming Gaussianity for the distributions for  $\beta$ . Recall the definition (45) of  $\bar{\sigma}^2$  and make the approximation  $\mathbf{H}\mathbf{B}\mathbf{H}^T\mathbf{R}^{-1} \approx \bar{\sigma}^2\mathbf{I}_P$ . Then the likelihood (47) can be written:

$$\begin{aligned} p(\mathbf{y}|\beta) &\propto \mathcal{N}(\mathbf{R}^{-1/2}\bar{\delta}|\mathbf{0}, (1 + \bar{\sigma}^2\beta)\mathbf{I}_P) \\ &\propto (1 + \bar{\sigma}^2\beta)^{-P/2} e^{-\|\bar{\delta}\|_{\mathbf{R}}^2/2(1 + \bar{\sigma}^2\beta)} \\ &\propto \chi^{+2}(\|\bar{\delta}\|_{\mathbf{R}}^2/P | (1 + \bar{\sigma}^2\beta), P). \end{aligned} \quad (51)$$

The value of  $\beta$  that maximizes this approximate likelihood is  $(\|\bar{\delta}\|_{\mathbf{R}}^2/P - 1)/\bar{\sigma}^2$ , i.e.  $\hat{\beta}_{\mathbf{R}}$  of equation (44).

The likelihood (51) may be further approximated by fitting the following shape to it:

$$p(\mathbf{y}|\beta) \approx \chi^{+2}(\hat{\beta}_{\mathbf{R}}|\beta, \hat{\nu}). \quad (52)$$

Irrespective of  $\hat{\nu}$ , the mode (in  $\beta$ ) is then the same as for equation (51), namely  $\hat{\beta}_{\mathbf{R}}$ . Also fitting the curvature at the mode to that of equation (51) yields  $\hat{\nu} = P[\bar{\sigma}^2\hat{\beta}_{\mathbf{R}}/(1 + \bar{\sigma}^2\hat{\beta}_{\mathbf{R}})]^2$ , corresponding to a variance (c.f. Table 2) equal to  $\hat{V}$  of equation (48), except for using  $\hat{\beta}_{\mathbf{R}}$  rather than  $\beta^f$ .

The benefit of the latter approximation (52) is the resulting conjugacy with an  $\chi^{-2}$  prior. Indeed, suppose the forecasted prior for the inflation parameter is:

$$p(\beta) = \chi^{-2}(\beta|\beta^f, \nu^f), \quad (53)$$

for some  $(\beta^f, \nu^f)$ . The posterior is then given by:

$$p(\beta|\mathbf{y}) = \chi^{-2}(\beta|\beta^a, \nu^a). \quad (54)$$

where

$$\nu^a = \nu^f + \hat{\nu}, \quad (55a)$$

$$\beta^a = (\nu^f\beta^f + \hat{\nu}\hat{\beta}_{\mathbf{R}})/\nu^a. \quad (55b)$$

This weighted-average update for the parameters is exactly that of the Kalman filter, except with slightly different meaning to the parameters. As such, it constitutes a natural and original derivation of the inflation filter of Miyoshi [2011].

## 4.3 Potential improvements

Rather than approximating the likelihood as  $\chi^{+2}$ , an improved approximation could be obtained by reverting to the likelihood  $p(\mathbf{y}|\beta)$  of equation (51) and directly fitting  $\chi^{-2}(\beta|\beta^a, \nu^a)$  to the posterior  $p(\mathbf{y}|\beta) \chi^{-2}(\beta|\beta^f, \nu^f)$  by matching their modes and local curvatures. As described for equation (50), fitting posterior criteria is the approach taken by Anderson [2007]. With the  $\chi^{-2}$  prior, though, an immediate benefit is that of precluding negative and nonsensical values for  $\beta^a$ . Moreover, it can be shown

that the posterior mode satisfies a cubic equation. The curvature is more complicated; alternatives include setting  $\nu^a = \nu^f + \nu$ , where  $\nu = \hat{\nu}$  or where  $\nu$  is such such that a likelihood  $\chi^{+2}(\hat{\beta}_{\mathbf{R}}|\beta, \nu)$  would yield the correct posterior mode.

The numerical approach offers another set of options: locating the mode by optimization and computing the curvature by finite differences. The latter could also be exchanged for the ratio of two points, as in Anderson [2007]. If such venues are pursued, it is then not necessary to make the approximation of reducing the likelihood (47) to (51); indeed, it is feasible to find the required statistics with the full likelihood, provided the pre-computed SVD, as in the EnKF- $N$ . However, this is not necessarily advisable, because it yields substantial bias due to the uncertainty in  $\bar{\mathbf{B}}$ , as discussed in appendix E.2.

An alternative approximation is to fit  $(\beta^a, \nu^a)$  via the mean and variance of the posterior, as computed by quadrature. This requires careful implementation to avoid a drift due to truncation errors, which otherwise accumulate exponentially through the DA cycles. It is also important to judiciously define the extent of the grid.

A related approach is to abandon the parametric approach altogether, and instead represent the posterior on a grid [e.g., Stroud *et al.*, 2016]. In the case of a single, global, inflation parameter, as in this paper, this approach is affordable for any purposeful precision. Finally, a Monte-Carlo representation can also be employed [e.g., Frei and Künsch, 2012].

For all variants, a choice must be made as to which point value of  $\beta$  to use to inflate the ensemble. Rather than using the parameter  $\beta^a$  directly, one can use the mean and mode (c.f. Table 2). Typically, though,  $\nu^a$  is so large that this does not matter much. Similarly, although  $\bar{\beta}_{\mathbf{R}}$  has a slight bias (appendix E.2), it “errs on the side of caution”. For this reason or other, de-biasing did not generally yield improvements in testing by twin experiments. Therefore, and for simplicity, de-biasing is not further employed.

#### 4.4 Specification of the variants shown in the comparative benchmarks

Several of the improvements of the previous subsection were tested with twin experiments. The results (not shown) indicate that most schemes, including the original one of section 4.2, perform surprisingly well (in terms of filter accuracy) provided they have reasonable settings of their tunable parameters. The most plausible explanation is that the inflation filters are consistent estimators: as the DA cycles build up, they all eventually converge towards a near-optimal value of inflation. In view of this parity it seems logical to opt for the simplest scheme, namely that of equations (54) and (55).

The forecast of  $\beta$  is also kept simple and pragmatic. It models the forgetting of past information, which is achieved by “relaxing” towards some background (and

initial) prior,  $\chi^{-2}(\beta|\beta_0, 0)$ , as follows:

$$p(\beta) = \chi^{-2}(\beta|\beta^f, \nu^f), \quad (56)$$

where

$$\nu^f = e^{-\Delta/L}\nu^a, \quad (57a)$$

$$\beta^f = e^{-\Delta/L}(\beta^a - \beta_0) + \beta_0, \quad (57b)$$

with  $\Delta$  as the time between analyses. The time scale  $L \geq 0$  controls the rate of relaxation, and could be set as a multiple of the time scale of the system. Alternatively, it can be set by solving the stationarity condition  $\nu_\infty = e^{-\Delta/L}\nu_\infty + \hat{\nu}$ , derived from equations (55a) and (57a).

Instead of equations (57a) and (57b), the numerical experiments use the fixed value  $\nu^f = 10^3$ , corresponding to a variance of approximately  $2(\beta^f)^2/10^3$ , according to Table 2. Moreover, instead of fitting it,  $\hat{\nu}$  was simply set to 1. Keeping  $\nu^f$  fixed is suboptimal in the spin-up phase of the twin experiments, but this part of the experiment is not included in the time-averaged statistics. Furthermore, keeping  $\nu^f$  fixed foregoes the interesting possibility of actually having the certainty decrease through an update, which can be observed to occur with the posterior fitting or non-parametric approaches. Nevertheless, this simplification was done (i) to facilitate reproduction; (ii) because in the twin experiments of this paper, the models and observational networks are homogeneous, and therefore using a variable  $\hat{\nu}$  is not so important; (iii) it was found that using the fitted  $\hat{\nu}$  sometimes yielded worse filter accuracy than keeping it fixed; (iv) to provide fair comparisons between all of the methods by equalizing the sophistication of their forecast step.

In addition to the adaptive inflation, Miyoshi [2011] also uses a fixed inflation of 1.015. This was tested and found to make little difference in the experiments herein. Without directly impacting its distribution, the value of the inflation actually applied to the ensemble is capped below by 0.9 for all methods. However, this clipping never occurred after the spin-up time of the experiment.

The above scheme is practically identical to that of Li *et al.* [2009], the differences having proven largely irrelevant and “cosmetic”, as discussed above. It is therefore labelled “ETKF adaptive”. Another scheme that was tested, labelled “EAKF adaptive”, is that of equation (50). Instead of fitting  $V^a$ , however, the value of  $V^f$  was fixed, and set (tuned) to 0.01. As described by Anderson [2007], the actual inflation applied to the ensemble is damped, using the value  $0.9\hat{\beta}_{\text{MAP}}$ . The above two schemes are the established standard in the literature, and have featured in many operational studies, although mainly in their spatialized formulations.

The proliferation of tunable “hyper-hyperparameters” (the hyperparameters of the inflation filter), is due to the hierarchical nature of adaptive filters, and may make the adaptive approach appear counterproductive. But, considering the breadth of error sources targeted, it should

be recognized that such methods will necessarily be ad-hoc, and that the existence of tuning parameters is to be expected. One should not be dismayed, however, because the performances of the adaptive filters are largely insensitive to the hyper-hyperparameter settings. Indeed, intuitively, more abstract parameters (further up the hierarchy) should have less impact, as is illustrated by the results of Roberts and Rosenthal [2001]. Indeed, the given values for the hyper-hyperparameters (i) were only tuned for a single experimental context, (ii) seem reasonable, and (iii) yield satisfactory filter accuracy almost universally across the experiments. Point (iii) corroborates previous findings [e.g., Anderson, 2007; Miyoshi, 2011], and suggests that these values may be used *in vivo*.

## 5 A hybrid EnKF- $N$

The EnKF- $N$  yields a form of adaptive inflation,  $\alpha_*$ . However, as it is built on the assumption that the truth is statistically indistinguishable from the ensemble, it only targets sampling error, and as such the prior for  $\alpha$  is always located nearby 1. The EnKF- $N$  is therefore not robust in the context of *model* error: when the model assumed by the filter differs from that of the truth (e.g., an incorrectly specified  $\mathbf{Q}$ ).

One way of dealing with model error is *tuned* inflation. If used in concert with the EnKF- $N$ , the tuned value could be seen as a measure of model error disentangled from sampling error, as suggested by Bocquet *et al.* [2013]. Here, however, the aim is to hybridize the EnKF- $N$  with an *adaptive* inflation scheme that estimates an inflation factor  $\beta$  targeted at model error. Notably, such a scheme has a prior that is time-dependent and generally not peaked around 1. The scheme used is the “adaptive ETKF” specified in section 4.4.

Consider

$$p(\mathbf{x}, \beta | \mathbf{y}) \propto p(\mathbf{y} | \mathbf{x}) p(\mathbf{x} | \beta) p(\beta). \quad (58)$$

In contrast to equation (46),  $p(\mathbf{x} | \beta)$  is here given by a scale mixture over  $\alpha$ , as in the pure EnKF- $N$  (7). In the current context, however,  $\bar{\mathbf{B}}$  is also scaled by  $\beta$ , i.e.  $p(\mathbf{x} | \alpha, \beta) = \mathcal{N}(\mathbf{x} | \bar{\mathbf{x}}, \alpha \beta \bar{\mathbf{B}})$ . Further, sampling error is assumed independent from model error:  $p(\alpha | \beta) = p(\alpha)$ . Hence, from equation (58):

$$p(\mathbf{x}, \beta | \mathbf{y}) \propto p(\mathbf{y} | \mathbf{x}) \left( \int p(\mathbf{x} | \alpha, \beta) p(\alpha) d\alpha \right) p(\beta). \quad (59)$$

Moving the likelihood inside as in the EnKF- $N$  (8) yields a mixture over  $p(\mathbf{y}, \mathbf{x} | \alpha, \beta)$ , which can be re-factorized to obtain:

$$p(\mathbf{x}, \beta | \mathbf{y}) \propto \left( \int p(\mathbf{x} | \mathbf{y}, \alpha, \beta) p(\mathbf{y} | \alpha, \beta) p(\alpha) d\alpha \right) p(\beta) \quad (60)$$

As in the EnKF- $N$  (9), the mixture is approximated by empirical Bayes:

$$p(\mathbf{x}, \beta | \mathbf{y}) \approx \underbrace{p(\mathbf{x} | \mathbf{y}, \alpha_*, \beta)}_{\approx p(\mathbf{x} | \mathbf{y}, \beta)} \left( \underbrace{\int p(\mathbf{y} | \alpha, \beta) p(\alpha) d\alpha}_{p(\mathbf{y} | \beta)} \right) p(\beta), \quad (61)$$

where  $p(\mathbf{x} | \alpha_*, \beta, \mathbf{y})$ , following the change of variables to  $\mathbf{w}$ , is given by equation (39) except that the prior covariance is now also scaled by  $\beta$ , which also impacts the selection of  $\alpha_*$  through the dual cost function.

The remaining integral of equation (61) is again approximated using a particular value of  $\alpha$ :

$$\int p(\mathbf{y} | \alpha, \beta) p(\alpha) d\alpha \approx p(\mathbf{y} | \alpha^f, \beta). \quad (62)$$

In this instance, however, the optimizing value of  $\alpha$  is not conditioned on  $\mathbf{y}$ , and is therefore denoted  $\alpha^f$ . In practice,  $\alpha^f = 1$  is used for simplicity. Thus,  $p(\mathbf{y} | \alpha^f, \beta)$  becomes the same as in equation (52), yielding the posterior of equation (54).

A final approximation is made to decouple the joint posterior: replacing  $\beta$  in the conditional distribution,  $p(\mathbf{x} | \mathbf{y}, \alpha_*, \beta)$ , by  $\beta_*$ , some point estimate from  $p(\beta | \mathbf{y}, \alpha^f)$ . This may again be seen as empirical Bayes, except that  $\beta$  is not a latent variable. Other reasons for only using a single inflation value for the ensemble are discussed in appendix D. The particular point used is the mean:

$$\beta_* = \frac{\nu^a}{\nu^a - 2} \beta^a. \quad (63)$$

Thus, equation (61) becomes:

$$p(\mathbf{x}, \beta | \mathbf{y}) \approx p(\mathbf{x} | \mathbf{y}, \alpha_*, \beta_*) p(\mathbf{y} | \alpha^f, \beta) p(\beta) \propto p(\mathbf{x} | \mathbf{y}, \alpha_*, \beta_*) p(\beta | \mathbf{y}, \alpha^f). \quad (64)$$

Algorithmically, the analysis update of the EnKF- $N$  hybrid can be stated as follows.

1. Update the general-purpose inflation,  $\beta$ , according to equations (55a) and (55b).
2. Conditional on  $\beta_*$  (63), find the EnKF- $N$  inflation using the dual (35):  $\alpha_* = \arg\min_{\alpha} D((N-1)/\beta_*\alpha)$ .
3. Update the ensemble by the ETKF with a prior inflation of  $\alpha_*\beta_*$ . In other words, implement equation (40) with  $(N-1)/\alpha_*\beta_*$  in place of  $\zeta_*$ .

Concerning the forecast, the decoupling of the posterior (64) means that the ensemble and general-purpose inflation  $\beta$  are independent. As shown in appendix F, the forecast of the ensemble can be treated separately from the forecast of  $\beta$ , namely equation (57). For the reasons described in section 4.4, however,  $\nu^f$  is fixed and set to  $\nu^f = 10^4$ , and  $\beta^f$  is set to the previous  $\beta^a$ . The EnKF- $N$  inflation,  $\alpha$ , is not forecasted, because it is not a filtering variable.

## 6 Benchmark experiments

The standard methods of section 4.4 and the hybrid of section 5 are tested with twin experiments: a synthetic truth and observation thereof are simulated and subsequently estimated by the DA methods. Contrary to the meaning of “twin”, however, the setup is deliberately one of model error: the model provided to the DA system is different from the one actually generating the truth.

The main system used is the two-scale/layer Lorenz model [Lorenz, 1996, 2005]. It constitutes a surrogate system for synoptic weather, exhibiting several of its characteristics, and allows for a study of the impact of unresolved scales on filter accuracy. The autonomous part is given by:  $\psi_i^\pm(\mathbf{u}) = u_{i\mp 1}(u_{i\pm 1} - u_{i\mp 2}) - u_i$ , where the indices apply periodically with the length of  $\mathbf{u}$ . Then

$$\frac{dx_i}{dt} = \psi_i^+(\mathbf{x}) + F - h\frac{c}{b}\sum_{j=1}^{10} z_{j+10(i-1)}, \quad i = 1, \dots, 36, \quad (65)$$

$$\frac{dz_j}{dt} = \frac{c}{b}\psi_j^-(bz) + 0 + h\frac{c}{b}x_{1+(j-1)//10}, \quad j = 1, \dots, 360, \quad (66)$$

where  $//$  means integer division. Unless otherwise stated, the constants are set as in Lorenz [1996]: time-scale ratio:  $c = 10$ , space-scale ratio:  $b = 10$ , coupling:  $h = 1$ , forcing:  $F = 10$ . The resulting dynamics, illustrated in Figure 3, are chaotic and have a leading Lyapunov exponent of 1.3775 [Mitchell and Carrassi, 2015].

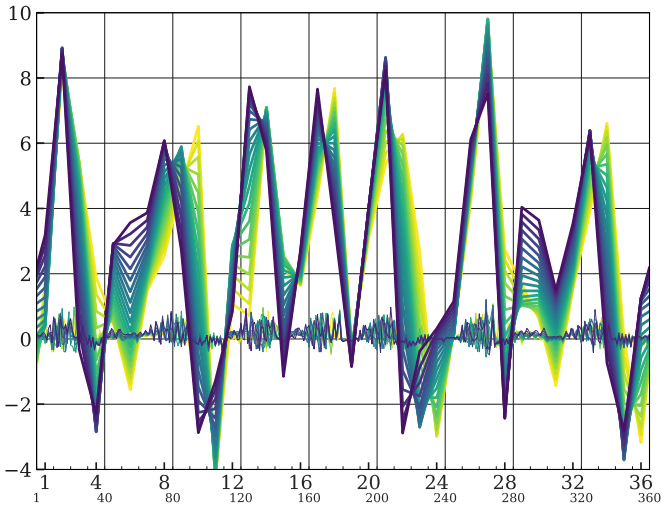


**Figure 3:** Illustration of the dynamics of the two-scale Lorenz model by 20 consecutive snapshots of the state profile. The colour gradation represents the time instances, which amount to a total time span of 0.3. The large-scale  $\mathbf{x}$  field with a mean value of 2.4 can be seen to be moving left. The small-scale  $\mathbf{z}$  field with a mean value of 0.1 is moving right; its variations are faster, but of less amplitude. The abscissa denotes the indices of (upper)  $\mathbf{x}$  and (lower)  $\mathbf{z}$ .

The truth is composed of both fields:  $[\mathbf{x}, \mathbf{z}]$ . By contrast, the model provided to the DA methods is a

truncated version of the full one:

$$\frac{dx_i}{dt} = \psi_i^+(\mathbf{x}) + F - [A + Bx_i], \quad i = 1, \dots, 36. \quad (67)$$

The term in the brackets parameterize (compensate for) the missing coupling to the small scale. Ahead of each experiment, the constants  $A$  and  $B$  are determined by linear regression to unresolved tendencies, as described by Wilks [2005]. The error parameterization removes the linear bias of the truncated model; this has been done because inflation is not well suited to deal with systematic errors. Higher-order parameterizations were tested and found to yield little improvement to the filter accuracies, while a 0-order parameterization yielded too much model error in the sense that most of the filter error is then due to the truncation rather than dynamical error growth.

Another source of model error is that the full model is integrated with a time step of 0.005, as necessitated by stiffness [Berry and Harlim, 2014], while the truncated model uses 0.05 to lower computational costs. However, this source of error was found to be negligible compared to the truncation itself.

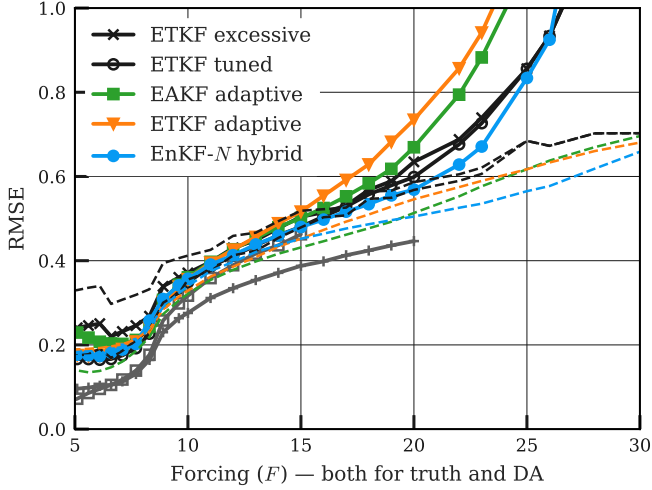
The time between observations is  $\Delta = 0.15$ . Direct observations are taken of the full  $\mathbf{x}$  with error covariance  $\mathbf{R} = \mathbf{I}_M$ . There is no model noise:  $\mathbf{Q} = \mathbf{0}$ . The filters are assessed by their accuracy as measured by root-mean squared error:

$$\text{RMSE} = \sqrt{\frac{1}{M}\|\mathbf{x} - \bar{\mathbf{x}}\|^2}, \quad (68)$$

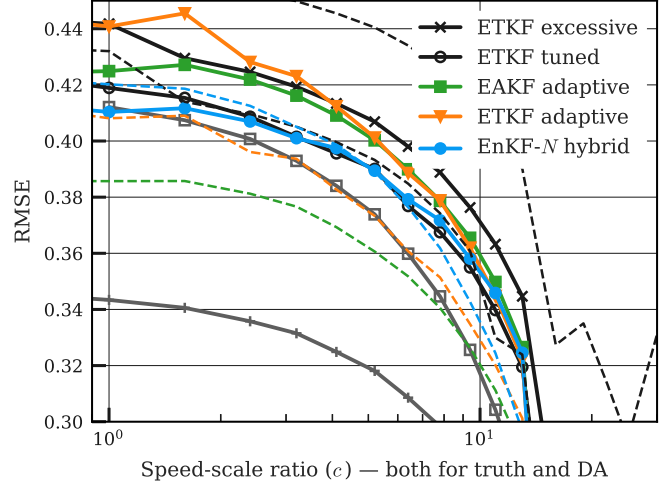
which is recorded immediately following each analysis. This instantaneous RMSE is then averaged in time (3300 cycles following a spin-up of 40 cycles), and over 32 repetitions of each experiment. A table of RMSE averages is compiled for a range of settings and presented as a figure. The figures also present (thin, dashed lines) the root-mean variances (RMS spread) of each method.

Figure (4a) shows benchmarks obtained with the two-scale system as a function of the forcing,  $F$ . The increasing RMSE averages of all filters reflect the fact (not shown) that the system variability and chaoticity both increase with  $F$ . The same applies for decreasing  $c$  in Figure (4b), where  $F$  is fixed at 10. Note that all of the adaptive filters are largely coincident at  $F = 10$  and  $c = 10$ , with RMSE scores almost as low as fixed, tuned inflation. This is because the hyper-hyperparameters for each method, described in section 4.4, were tuned at this point (and this point only). By contrast, the fixed inflation of the “ETKF tuned” filter is determined for each system and setting by selecting for the lowest RMSE among 40 inflation values between 0.98 and 3, most of which are close to 1.

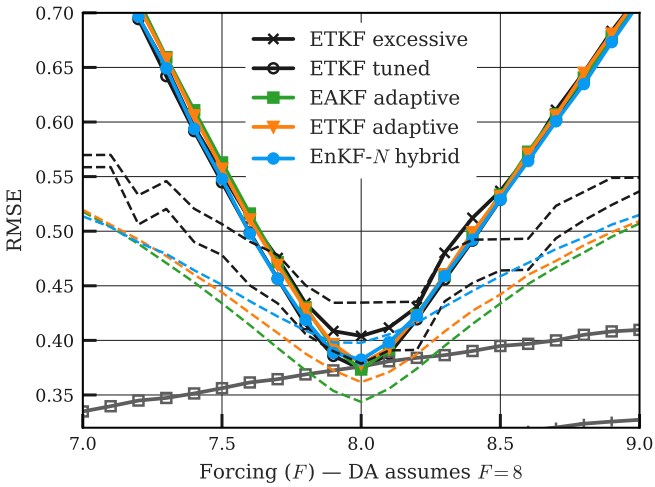
It is not very surprising that tuning an adaptive filter will make it about as accurate as possible. The objective, however, is to avoid any tuning. What is surprising is how well all of the adaptive filters perform overall. Indeed, except for the fairly extreme contexts of  $F > 15$  or  $c < 4$ , the difference in RMSE is small in the sense that the



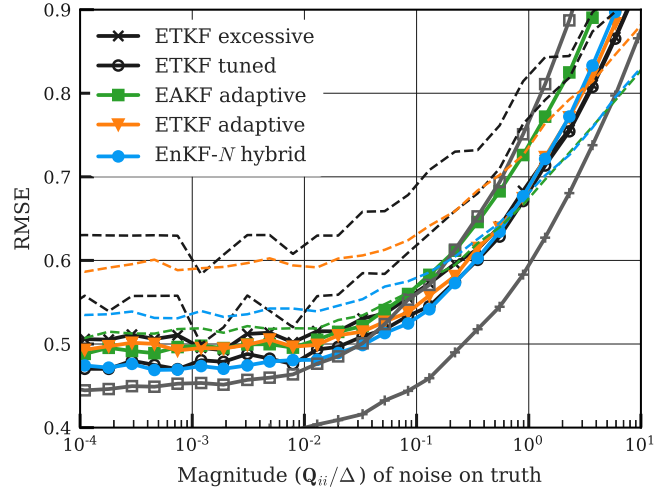
(a) From the two-scale system, with  $N = 20$ .



(b) From the two-scale system, with  $N = 20$ .



(c) From the single-scale system, with  $N = 20$ .



(d) From the Lorenz-63 system, with  $N = 3$ .

**Figure 4:** Accuracy benchmarks of the adaptive inflation filters, plotted as functions of various control variables. Also included in the plots is the RMS spread, plotted as thin, dashed lines. For perspective, two baselines are provided, in grey. These are obtained with the full (i.e. perfect) model using the pure EnKF- $N$ : one with the same ensemble size as the adaptive filters (marker:  $\square$ ), and one with  $N = 80$  (marker:  $+$ ). Among the adaptive methods, the proposed hybrid EnKF- $N$  (blue) scores the lowest RMSE averages nearly systematically across all contexts, albeit by a moderate margin.

adaptive filters are all superior to “ETKF excessive”: a fixed-inflation filter with a suboptimal inflation factor that adds 0.1 to the optimal value.

Benchmarks were also obtained with the single-scale system, where both the truth and the DA systems are given by:

$$\frac{dx_i}{dt} = \psi_i^+(\mathbf{x}) + F, \quad i = 1, \dots, 40, \quad (69)$$

and there is no  $\mathbf{z}$  field. As in Anderson [2007], the model error consists in using a different value of  $F$  for the truth than for the DA system. The setup is otherwise repeated. As shown in Figure (4c), the benchmarks plotted as a function of  $F$  are V-shaped, with the lowest scores obtained in the absence of error ( $F = 8$ ). The adaptive filters score very similar RMSE averages, which are generally significantly in excess of the RMS spread scores. The mismatch can be explained by the well known bias-variance decomposition of RMSE, and the fact that the model error contains significant bias. The presence of bias is also a likely cause for the similarity of the RMSE averages of the adaptive methods, because inflation is not well suited to treat bias.

Tests were also run with the 3-variable Lorenz-63 system [Lorenz, 1963], where the model error consists in adding independent white noise to the truth. The setup is the same as above, except that  $\mathbf{R} = 2\mathbf{I}_3$ . Figure (4d) shows the corresponding benchmarks. These are obtained with a small ensemble ( $N = 3$ ); using a larger ensemble, the relative advantage of the hybrid disappears.

The hybrid EnKF- $N$  obtains slightly superior accuracy than the adaptive ETKF and EAKF for nearly all experiments. This is as expected from theory: separate, dedicated treatment of sampling and model errors yield improved accuracy. The advantage of the hybrid is apparent in the illustrative time series of the inflation and other statistics shown by Figure 5 where, notably, the inflation of the hybrid EnKF- $N$  has much more volatility (time-variability). Because their inflation factors are not anchored to 1, this volatility cannot be reproduced by the adaptive ETKF and EAKF without much more lenient settings of  $\nu^f$  (or  $V^f$ ), which would yield excessive longer-term volatility. On the other hand, the volatility also means that larger inflation values will occur. Since inflation is not a physical or especially gentle way of increasing spread, this could potentially cause trouble.

Different hyper-hyperparameter values for the adaptive EAKF and ETKF will penalize their RMSE scores for some settings, and reward it for other settings. This sensitivity was observed to be much reduced for the hybrid, which is in line with the principal objective: to avoid tuning across a multitude of contexts.

A secondary objective is to obtain improved accuracy compared to fixed, tuned inflation, as has been previously observed for the pure EnKF- $N$  in the perfect-model context [Boc12]. Figure 4 shows that this is sometimes achieved, but by a very small margin.

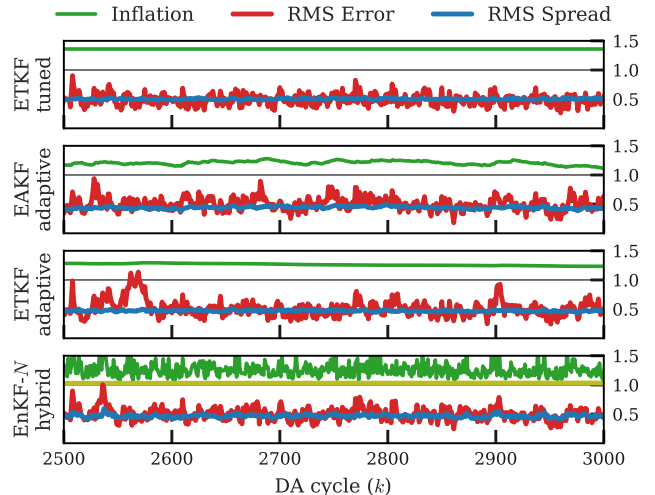


**Figure 5:** Illustration of the statistics from the twin experiments by a segment of the typical time series. Generated with the two-scale Lorenz model, with  $F = 16$ . In the panel of the hybrid EnKF- $N$ , the second inflation line (yellow) indicates the value of  $\beta^a$ , and averages 1.02.

Further experiments (not shown) were carried out, using different ensemble sizes and other types of model errors. The trends were similar to the benchmarks already shown and discussed, but typically with less relative difference between the filters.

## 7 Concluding remarks

This paper has developed an adaptive inflation scheme that is a hybrid of the finite-size ensemble Kalman filter [the EnKF- $N$  of Boc11; Boc15; Boc12] and the estimator conventionally associated with the ensemble transform Kalman filter (ETKF), namely  $\hat{\beta}_{\mathbf{R}}$ . In so doing, it has provided several novel theoretical insights pertaining to the EnKF and the EnKF- $N$ .

Motivated by two univariate toy experiments, section 2.1 and appendix B showed the connection between nonlinearity and sampling error. Section 2.2 then gave a detailed and explicit catalogue of the circumstances for inflation, including linearity, stochasticity, and ensemble size; it was also discussed why the choice of normalization such as  $\frac{1}{N-1}$  is not crucial, and why the bias in  $\bar{\mathbf{P}}^a$  does not lead to collapse nor necessarily divergence. Next, section 3.1 gave an introductory explanation of how (e.g., empirical Bayes) and why (e.g., feedback) the EnKF- $N$  works. Section 3.4 showed how the effective prior of the EnKF- $N$  reduces to a Gaussian scale mixture, again demonstrating the relationship between sampling error and inflation. Section 3.6 used a saddle-point method to retain the inflation-centric expressions all the way up to the posterior. Without recourse to Lagrangian duality theory, section 3.7 then finalized the re-derivation of the dual EnKF- $N$  by showing how the mode of the posterior may be found by optimizing over the inflation factor,  $\alpha$ .



Section 4 presented a formal and unifying survey of the existing adaptive inflation literature, generally aimed at model error as well as sampling error. Particular attention was given to the schemes conventionally associated with the EAKF and the ETKF ( $\beta_{\mathbf{R}}$ ). The ETKF scheme was also re-derived in section 4.2 in a more natural and rigorous manner using the  $\chi^{-2}$  distribution. Several potential improvements, some novel, were discussed in section 4.3, but generally found to be less rewarding than hoped for. The survey is supplemented by appendix D, which shows how an inflation estimator may be obtained from variational Bayes, and appendix E, whose analysis contains some results on bias and maximum likelihood. Appendix F comments on the forecasting of hyperparameters such as the inflation parameter  $\beta$ , attempting to provide theoretical models and justifications as called for in the existing inflation literature.

Building on the above, section 5 developed a hybrid between the EnKF- $N$  and the adaptive ETKF inflation scheme. The hybrid employs two inflation factors,  $\alpha$  and  $\beta$ , separately targeting sampling and model error, respectively. The EnKF- $N$  component ( $\alpha$ ) adds negligible computational cost and no further tuning parameters, yet increases the flexibility and thus ability of the inflation scheme, as illustrated by the time-variability of the hybrid's inflation. The experiments of section 6 showed that the hybrid has improved filter accuracy compared to pre-existing methods. However, the improvement was found to be relatively minor, as was the difference in accuracy between the existing methods. This seems surprising in view of the essential importance of inflation in some configuration of the EnKF. Part of the explanation may be that, as a hyperparameter, the accuracy of the inflation estimates is not as important as that of the (primary) state variables and that, instead, the main importance of the inflation scheme consists in its capacity to avoid divergence occurrences, which is a matter of a more boolean character. Another part of the reason is that the inflation estimates converge and become nearly constant within a relatively short span of time, and that these asymptotic estimates are sufficiently accurate for all of the methods.

With regards to other and larger application cases, the hybrid EnKF- $N$  may yield improved filtering performance compared to standard ETKF and EAKF adaptive inflation schemes. Spatialization should be implemented as in Miyoshi [2011], associating each local domain with its own inflation parameter. However, considering the above experimental findings, it is questionable whether the improvement of the hybrid is sufficient to merit its implementation, unless the context is strongly nonlinear or the ensemble size is very small. This suggests the conclusion, afforded by the rigour and scope of this paper, that further sophistication of adaptive inflation schemes is unlikely to yield significant improvements in filter accuracy.

## A Standard distributions

Consult Table 2 for the specifications of the distributions in use. The following properties are also of use.

**Property 1** The (“scaled”) chi-square distribution is equivalent to the Gamma distribution:

$$\chi^{\pm 2}(\beta|s, \nu) = \text{Gamma}^{\pm 1}(\beta|\nu/2, \nu s^{\mp 1}/2), \quad (70)$$

where the switch sign  $\pm$  has been used to represent both the regular and inverse distributions. The  $\chi$  parameterization has been preferred for the notational simplicity of the relations of Properties 2 to 4.

**Property 2** Asymptotic normality. If  $\beta \sim \chi^{\pm 2}(s, \nu)$ , then the distribution of  $\sqrt{\nu}(\beta - s)$  converges to  $\mathcal{N}(0, 2s^2)$  as  $\nu \rightarrow \infty$ . This shows that  $s$  is a location parameter, while  $2s^2/\nu$  plays the role of variance, which is why this paper prefers referring to  $\nu$  as “certainty” instead of “degree of freedom”. The asymptotic result for  $\chi^{+2}$  is a well known consequence of the central limit theorem, since  $\beta$  may then be written as an average of random variables. The result for  $\chi^{-2}$  is less known, but can be shown by through the pointwise convergence of the pdf of  $\sqrt{\nu}(\beta - s)$ , normalized by its value at 0.

**Property 3** In the univariate case ( $M = 1$ ),

$$\mathcal{W}^{\pm 1}(\beta|s, \nu) = \chi^{\pm 2}(\beta|s, \nu). \quad (71)$$

**Property 4** Reciprocity. If  $t = 1/\beta$ :

$$\begin{aligned} p(\beta) &= \chi^{-2}(\beta|s, \nu) \\ \iff p(t) &= \chi^{+2}(t|1/s, \nu). \end{aligned} \quad (72)$$

**Property 5** Reciprocity. If  $\mathbf{T} = \mathbf{B}^{-1}$ :

$$\begin{aligned} p(\mathbf{B}) &= \mathcal{W}^{-1}(\mathbf{B}|\mathbf{S}, \nu) \\ \iff p(\mathbf{T}) &= \mathcal{W}^{+1}(\mathbf{T}|\mathbf{S}^{-1}, \nu), \end{aligned} \quad (73)$$

as follows by the change of variables and the Jacobian  $|\mathbf{T}|^{-(M+1)}$  [Muirhead, 1982, §. 2.1].

**Property 6** Let  $\mathbf{u} \neq \mathbf{0}$  be any  $m$ -dimensional vector, or an (almost never zero) random vector. If  $\mathbf{T} \sim \mathcal{W}^{+1}(\mathbf{S}, \nu)$  is independent of  $\mathbf{u}$ , then

$$\frac{\mathbf{u}^{\top} \mathbf{T} \mathbf{u}}{\mathbf{u}^{\top} \mathbf{S} \mathbf{u}} \sim \chi^{+2}(1, \nu). \quad (74)$$

Moreover, this statistic is also independent of  $\mathbf{u}$ . Proof: Theorem 3.2.8 of Muirhead [1982].

**Table 2:** Parametric probability distributions. As elsewhere in the paper,  $\mathbf{b}, \mathbf{x} \in \mathbb{R}^M$ ,  $\mathbf{B}, \mathbf{S} \in \mathcal{B}$ ,  $s, \beta > 0$ , and it is assumed that  $\nu > M$ . The constants are  $c_{\mathcal{N}} = (2\pi)^{-M/2}$ ,  $c_t = \frac{\Gamma(\frac{\nu+M}{2})}{(\pi\nu)^{M/2}\Gamma(\nu/2)}$ ,  $c_{\mathcal{W}} = \frac{\nu^{\nu/2}}{2^{\nu M/2}\Gamma_M(\nu/2)}$ , and  $c_{\chi} = c_{\mathcal{W}}$  with  $M = 1$ . The (unlisted) variance of element  $(i, j)$  of  $\mathbf{B}$  with the Wishart distribution is  $(s_{ij}^2 + s_{ii}s_{jj})/\nu$ , where  $s_{ij}$  is element  $(i, j)$  of  $\mathbf{S}$ . The variances of the inverse-Wishart distribution are asymptotically, for  $\nu \rightarrow \infty$ , the same.

Name	Symbol	Probability density function	Mean	Mode	(Co)Var
Gauss./Normal	$\mathcal{N}(\mathbf{x} \mathbf{b}, \mathbf{B})$	$= c_{\mathcal{N}}  \mathbf{B} ^{-1/2} \exp(-\frac{1}{2}\ \mathbf{x} - \mathbf{b}\ _{\mathbf{B}}^2)$	$\mathbf{b}$	$\mathbf{b}$	$\mathbf{B}$
$t$ distribution	$t(\mathbf{x} \nu; \mathbf{b}, \mathbf{B})$	$= c_t  \mathbf{B} ^{-1/2} (1 + \frac{1}{\nu}\ \mathbf{x} - \mathbf{b}\ _{\mathbf{B}}^2)^{-(\nu+M)/2}$	$\mathbf{b}$	$\mathbf{b}$	$\frac{\nu}{\nu-2}\mathbf{B}$
Wishart	$\mathcal{W}^{+1}(\mathbf{B} \mathbf{S}, \nu)$	$= c_{\mathcal{W}}  \mathbf{S} ^{-\nu/2}  \mathbf{B} ^{(\nu-M-1)/2} e^{-\text{tr}(\nu\mathbf{B}\mathbf{S}^{-1})/2}$	$\mathbf{S}$	$\frac{\nu-M-1}{\nu}\mathbf{S}$	
Inv-Wishart	$\mathcal{W}^{-1}(\mathbf{B} \mathbf{S}, \nu)$	$= c_{\mathcal{W}}  \mathbf{S} ^{\nu/2}  \mathbf{B} ^{-(\nu+M+1)/2} e^{-\text{tr}(\nu\mathbf{S}\mathbf{B}^{-1})/2}$	$\frac{\nu}{\nu-M-1}\mathbf{S}$	$\frac{\nu}{\nu+M+1}\mathbf{S}$	
Chi-square	$\chi^{+2}(\beta s, \nu)$	$= c_{\chi} s^{-\nu/2} \beta^{\nu/2-1} e^{-\nu\beta/2s}$	$s$	$\frac{\nu-2}{\nu}s$	$2s^2/\nu$
Inv-chi-sq.	$\chi^{-2}(\beta s, \nu)$	$= c_{\chi} s^{\nu/2} \beta^{-\nu/2-1} e^{-\nu s/2\beta}$	$\frac{\nu}{\nu-2}s$	$\frac{\nu}{\nu+2}s$	$\frac{2(\nu s)^2}{(\nu-2)^2(\nu-4)}$

## B Why does nonlinearity generate sampling error?

This discussion complements that of section 2.

A sample does not *per se* have a ‘‘sampling error’’; it is by definition random, i.e. subject to variation. By contrast, estimators, or rather their realized estimates, have sampling error: the difference between the estimate and its expected value. By extension, any statistic (any function of the sample) may be said to have sampling error; for simplicity, however, the discussion below is limited to the non-central sample moments, i.e.  $\hat{\mu}_m(\{x_n\}_{n=1}^N) = N^{-1} \sum_{n=1}^N x_n^m$ , in the univariate case. If the sample is drawn from the same distribution as  $x$ , then  $\hat{\mu}_m$  is an unbiased estimate of  $\mu_m = \mathbb{E}[x^m]$ , the  $m$ -th moment of  $x$ , and the sampling error is the difference

$$\text{Error}_m = \hat{\mu}_m - \mu_m. \quad (75)$$

The moments become coupled through the forecast dynamics,  $\mathcal{M}$ . This is revealed by the Taylor-expansion analysis used to derive higher-order extended Kalman filters [e.g., Einicke, 2012, §8]. For example, if (locally to the support of  $p(x)$ ) the model  $\mathcal{M}$  can be represented by a polynomial of degree  $d$ , then the  $m$ -th moment of the random variable  $\mathcal{M}(x)$  is a linear combination of moments of  $x$  of order 1 through  $md$ :

$$\mu_m^f = \sum_{i=1}^{md} C_{m,i} \mu_i. \quad (76)$$

Thus, for  $d > 1$  the moments get mixed and, in particular, impacted by moments of higher order. But in the linear case ( $d = 1$ ) the moments stay decoupled:  $C_{m,i} = 0$  unless  $i = m$ , and so  $\mu_m^f = \mathbf{M}^m \mu_m$ , where  $\mathbf{M}$  is the (scalar) linear model. To wit, an important property of the Kalman filter is that the covariance evolution is independent of the mean evolution.

A similar analysis reveals that the same coupling takes place for the sample moments,  $\hat{\mu}_m$ . Therefore the sampling errors are also coupled:

$$\text{Error}_m^f = \sum_{i=1}^{md} C_{m,i} \text{Error}_i. \quad (77)$$

But an  $N$ -sized ensemble can only match  $N$  moments, e.g.,  $\text{Error}_i = 0$  for  $i = 1, \dots, N$ . Thus there will always be some sampling error present for  $i > N$ , and this will cascade into the lower-order forecast errors. In summary, non-linearity causes sampling error in (e.g.) the mean and covariance by pulling in the inevitable (with finite  $N$ ) sampling error from higher-order moments.

The above analysis is concerned with the *generation* of sampling error. Another reason for sampling error in the context of nonlinearity is that chaos prevents its *elimination* by limiting the effect of far-past observations (as opposed to the linear case illustrated in Figure 1, where the initial sampling error is quickly attenuated). It is not immediately clear whether this is a separate cause or, rather, a different perspective on the same phenomenon.

## C Alternative proof for section 3.4

Boc11 showed that the covariance mixture of the effective prior integrates to the  $t$  distribution. But section 3.6 showed that the scale mixture also integrates to the  $t$  distribution. Thus the simplest way to prove the reduction from the covariance to the scale mixture is just to note this equivalence. However, this is of limited pedagogical value.

A more explicit proof is given in the following. To simplify notations, let  $\nu = N - 1$  and  $\mathbf{S} = \varepsilon_N \bar{\mathbf{B}}$ , use the change of variables  $\mathbf{B}' = \varepsilon_N \mathbf{B}$ , and set (without loss of generality)  $\bar{\mathbf{x}} = \mathbf{0}$ . Equation (17) then becomes:

$$p(\mathbf{x}|\mathbf{E}) = \int_{\mathcal{B}} d\mathbf{B} \mathcal{N}(\mathbf{x}|\mathbf{0}, \mathbf{B}) \mathcal{W}^{-1}(\mathbf{B}|\mathbf{S}, \nu). \quad (78)$$

Recall the expression of the Dirac delta by the Fourier transform:  $\delta(x) = \int_{\mathbb{R}} dz e^{-2\pi izx}$ . Thus one can write  $e^{-\|\mathbf{x}\|_{\mathbf{B}}^2/2} \propto \int_{\tau>0} d\tau \int_{\mathbb{R}} dz e^{-\tau/2} e^{iz(\tau - \|\mathbf{x}\|_{\mathbf{B}}^2)/2}$  and hence

$$p(\mathbf{x}|\mathbf{E}) \propto \int_{\tau>0} d\tau e^{-\tau/2} \int_{\mathbb{R}} dz e^{iz\tau/2} \int_{\mathbf{B}} d\mathbf{B} |\mathbf{B}|^{-(\nu+m+2)/2} e^{-\text{tr}(\Sigma\mathbf{B}^{-1})/2}, \quad (79)$$

where  $\Sigma = \nu\mathbf{S} + iz\mathbf{x}\mathbf{x}^\top$ . The innermost integrand can be recognized as a Wishart pdf. As shown in Boc11, it integrates to a  $t$  distribution in  $\mathbf{x}$ :

$$p(\mathbf{x}|\mathbf{E}) \propto \int_{\tau>0} d\tau e^{-\tau/2} \int_{\mathbb{R}} dz e^{iz\tau/2} \left(1 + \frac{iz}{\nu} \|\mathbf{x}\|_{\mathbf{S}}^2\right)^{-(\nu+1)/2}. \quad (80)$$

The integral over  $z$  can be calculated using the formula  $\int_{\mathbb{R}} dz e^{iza}(1+izb)^{-k} \propto b^{-k} e^{-a/b} a^{k-1}$ , which can be obtained using the contour of the infinite semi-circle enclosing the upper complex plane except for a keyhole incision down along the vertical branch cut to  $i/b$ , tightly around it, and back up. This yields:

$$p(\mathbf{x}|\mathbf{E}) \propto \int_{\tau>0} d\tau e^{-\tau/2} (\|\mathbf{x}\|_{\mathbf{S}}^2/\nu)^{-(\nu+1)/2} e^{-\tau\|\mathbf{x}\|_{\mathbf{S}}^2/2\nu} (\tau/2)^{(\nu-1)/2}, \quad (81)$$

and with the change of variables  $\tau = \|\mathbf{x}\|_{\mathbf{S}}^2/s$ ,

$$p(\mathbf{x}|\mathbf{E}) \propto \int_{s>0} ds \mathcal{N}(\|\mathbf{x}\|_{\mathbf{S}}|0, s) \chi^{-2}(s|1, \nu). \quad (82)$$

## D Joint state-covariance estimation

The joint approach approximates  $p(\mathbf{x}, \beta|\mathbf{y})$  simultaneously in  $\mathbf{x}$  and  $\beta$  such that their analyses impact each other. Because of its non-Gaussianity, this is particularly relevant for state-covariance or state-inflation estimation. A common solution is to use variational methods for parametric fitting. As detailed below, this leads to iterative schemes where the update to the hyperparameter,  $\beta$ , is computed in terms of the updated ensemble (for  $\mathbf{x}$ ), and vice versa. Note that some of the literature below is concerned with estimating  $\mathbf{R}$  (jointly with  $\mathbf{x}$ ), but is still pertinent by the proximity of the problem to that of estimating  $\mathbf{B}$ .

Instead of the variational approach, a more principled approach is to obtain the marginal  $p(\beta|\mathbf{y})$  and sample it. This yields a hyper-ensemble and an implied ensemble of distributions  $p(\mathbf{x}|\beta, \mathbf{y})$ . The label ‘‘hierarchical’’ is sometimes reserved for adaptive filters treating the hyperparameter in this more Bayesian manner. A

criticism is that it could cause discrete jumps between localization domains. Furthermore, if only a single  $\mathbf{x}$  is drawn from  $p(\mathbf{x}|\beta, \mathbf{y})$  for each  $\beta$  (i.e. not using an ensemble of ensembles) then it seems especially prone to spurious correlations. Myrseth *et al.* [2010] provided one example of a hierarchical EnKF, but without conditioning the hyperparameter on  $\mathbf{y}$ , without accounting for model error, and with a forecast of (the hyperprior of)  $\mathbf{B}$  that decays towards  $\mathbf{0}$ . Tsyrlunikov and Rakitko [2015] present an ambitious hierarchical EnKF, explicitly considering both model and sampling error. However, the filter is only tested in experiments with a novel, univariate model.

An intriguing approach is that of Stroud and Bengtsson [2007]. They peg the scaling of  $\mathbf{R}$  and  $\mathbf{Q}$  together, so as to estimate only a single parameter,  $\beta$ . This is difficult to justify, but simplifies the problem significantly because then  $\bar{\mathbf{B}}$  also scales with  $\beta$  (provided linear dynamics) so that  $p(\mathbf{x}, \beta) = \mathcal{N}(\mathbf{x}|\bar{\mathbf{x}}, \beta\bar{\mathbf{B}}) \chi^{-2}(\beta|\dots)$  is conjugate to  $p(\mathbf{y}|\mathbf{x}, \beta)$ , and the joint posterior is available in closed form, with trivial parametric updates. However, without pegging  $\mathbf{Q}$  to  $\mathbf{R}$ , the conjugacy is lost.

Sarkka and Hartikainen [2013]; Sarkka and Nummenmaa [2009] introduce the Variational Bayes (VB) method to deal with the non-conjugacy. Nakabayashi and Ueno [2017] apply the same method in the framework of the EnKF. The VB method imposes an approximate posterior with two factor distributions,  $q(\mathbf{x}|\mathbf{y})q(\mathbf{R}|\mathbf{y})$ , fitted by minimizing the Kullback-Leibler divergence from the correct posterior,  $p(\mathbf{x}, \mathbf{R}|\mathbf{y})$ . This yields the condition that each factor be the (geometric) marginal of  $p(\mathbf{x}, \mathbf{R}|\mathbf{y})$  with respect to the other, i.e. two coupled pdf equations. Independence is assumed for the prior:  $p(\mathbf{x}, \mathbf{R}) = \mathcal{N}(\mathbf{x}|\bar{\mathbf{x}}, \bar{\mathbf{B}}) \mathcal{W}^{-1}(\mathbf{R}|\mathbf{R}^f, \nu^f)$ . It is then shown that the distributions of the approximate posterior are again  $\mathcal{N}$  and  $\mathcal{W}^{-1}$ , with parameters computable by fixed point iteration. Iteration  $i + 1$  consists of the EnKF equations using the  $i$ -th estimate of  $\mathbf{R}^a$  to compute the analysis mean,  $\bar{\mathbf{x}}^a$ , and covariance,  $\bar{\mathbf{P}}^a$ , whose updated values are then used to in the update  $\mathbf{R}^a = \{\nu^f \mathbf{R}^f + \hat{\mathbf{R}}\}/\nu^a$  where  $\nu^a = \nu^f + 1$  and

$$\hat{\mathbf{R}} = (\mathbf{y} - \mathbf{H}\bar{\mathbf{x}}^a)(\mathbf{y} - \mathbf{H}\bar{\mathbf{x}}^a)^\top + \mathbf{H}\bar{\mathbf{P}}^a\mathbf{H}^\top. \quad (83)$$

Ueno and Nakamura [2016], also estimating  $\mathbf{R}$  in the framework of the EnKF, use the expectation maximization method to maximize the marginal posterior  $p(\mathbf{R}|\mathbf{y})$ , with an  $\mathcal{W}^{-1}$  prior. The expectation is over  $\mathbf{x}$  given  $\mathbf{y}$  and the current estimate of  $\mathbf{R}$ , where the empirical distribution is assumed for the prior:  $p(\mathbf{x}) \approx N^{-1} \sum_n \delta(\mathbf{x} - \mathbf{x}_n)$ . This yields iterations involving weighted statistics. A cursory investigation indicates that if, instead, the standard EnKF assumption had been used:  $p(\mathbf{x}) \approx \mathcal{N}(\mathbf{x}|\bar{\mathbf{x}}, \bar{\mathbf{B}})$ , then the method would have yielded iterations as in equation (83). This similarity is perhaps unsurprising in view of the close connection to the VB method.

An original result is obtained by applying the VB method to estimate the inflation parameter. It uses the

prior  $p(\mathbf{x}, \beta) = \mathcal{N}(\mathbf{x}|\bar{\mathbf{x}}, \beta\bar{\mathbf{B}}) \chi^{-2}(\beta|\beta^f, \nu^f)$ , which includes a dependency between  $\mathbf{x}$  and  $\beta$ . It can then be shown that the resulting VB scheme uses the  $i$ -th iterate of  $\beta^a$  to compute the  $i+1$  iterates of  $\bar{\mathbf{x}}^a$  and  $\bar{\mathbf{P}}^a$  which, in turn, are used to compute the  $i+1$  iterate  $\beta^a = \{\nu^f\beta^f + \hat{\beta}\}/\nu^a$  where  $\nu^a = \nu^f + m$  and

$$\hat{\beta} = \|\bar{\mathbf{x}}^a - \bar{\mathbf{x}}^f\|_{\bar{\mathbf{B}}}^2 + \text{tr}(\bar{\mathbf{P}}^a\bar{\mathbf{B}}^{-1}), \quad (84)$$

which should be computed in the ensemble subspace if  $N \leq m$ . Note that this scheme could almost have been anticipated by comparing to equation (83) and the trigonometric relations developed in Desroziers *et al.* [2005] (see their Figure 1).

## E More on marginal inflation estimators

Equation (42) has also been derived and analysed in the variational (non-Kalman) framework by Chapnik *et al.* [2006]; Desroziers and Ivanov [2001]; Ménard [2016], where it is seen as a consistency criterion on the cost function. Further diagnostics, employing distances labelled “observation-analysis” and “analysis-background” were also derived, enabling the simultaneous estimation of the observation error covariance. Li *et al.* [2009] make use of this in an ensemble framework, as do Kotsuki *et al.* [2017]; Ying and Zhang [2015], who makes use of the scheme in a “relaxation” variety. However, the following focuses again on the “observation-background” statistic that is equation (42), and some other estimators thereof.

### E.1 Other variants

It is common to form chi-square diagnostics by measuring  $\bar{\boldsymbol{\delta}}$  by its Mahalanobis norm [Haussaire, 2017; Ménard *et al.*, 2000; Wu *et al.*, 2013]. This provides the motivation to use  $\bar{\mathbf{C}}(1)^{-1}$  to transform equation (42), yielding:

$$\hat{\beta}_{\bar{\mathbf{C}}} := \frac{\|\bar{\boldsymbol{\delta}}\|_{\bar{\mathbf{C}}(1)}^2 - \text{tr}(\mathbf{R}\bar{\mathbf{C}}(1)^{-1})}{\text{tr}(\mathbf{H}\bar{\mathbf{B}}\mathbf{H}^T\bar{\mathbf{C}}(1)^{-1})}. \quad (85)$$

Alternatively, equation (42) can be transformed by  $(\mathbf{H}\bar{\mathbf{B}}\mathbf{H}^T)^{-1}$ , yielding  $(\bar{\boldsymbol{\delta}}\bar{\boldsymbol{\delta}}^T - \mathbf{R})(\mathbf{H}\bar{\mathbf{B}}\mathbf{H}^T)^{-1} = \beta\mathbf{I}_P$ . For the purpose of inflation, this seems like the best option because then the trace consists of terms with the same expected magnitude, yielding the lowest aggregate variance. The estimator becomes:

$$\hat{\beta}_{\mathbf{H}\bar{\mathbf{B}}\mathbf{H}^T} := \frac{1}{P} \{ \|\bar{\boldsymbol{\delta}}\|_{\mathbf{H}\bar{\mathbf{B}}\mathbf{H}^T}^2 - \text{tr}(\mathbf{R}(\mathbf{H}\bar{\mathbf{B}}\mathbf{H}^T)^{-1}) \}, \quad (86)$$

If  $\mathbf{H}\bar{\mathbf{B}}\mathbf{H}^T$  is rank-deficient, then  $\hat{\beta}_{\mathbf{H}\bar{\mathbf{B}}\mathbf{H}^T}$  must be defined using the pseudo-inverse. The estimate would then not be impacted by components of  $\bar{\boldsymbol{\delta}}$  outside of the ensemble subspace, something which seems beneficial in light of the discussion of §5 of section 2.2.

None of the listed estimators are computationally costly, because they can all be computed in terms of the SVD  $[(N-1)\mathbf{R}]^{-1/2}\mathbf{Y} = \mathbf{U}\text{diag}(\sigma_1, \dots, \sigma_P)\mathbf{V}^T$ , which has already been computed for doing the ETKF update.

### E.2 Single-cycle bias

This section is concerned with the properties of the estimators in a single analysis, meaning that the priors and posteriors do not intervene. It should be recognized that section 4.1 implicitly assumes that the ensemble size is infinite. Thus  $\varepsilon_N$  could be ignored, and the state distributions were assumed Gaussian, rather than  $t$ . In actuality, however, the biases are largely due to the finite size of  $N$ , which yields uncertainty in  $\bar{\mathbf{B}}$ . To investigate this, the following assumes that the ensemble truly is sampled as in equation (5), except for some scaling of the covariance,  $\beta > 0$ .

Using the SVD quantities, it can be shown that each of the previously listed estimators of  $\beta$  satisfy the condition:

$$0 = \sum_{i=1}^P \gamma_i (1 + \hat{\beta}\sigma_i^2 - d_i^2), \quad (87)$$

where  $d_i$  is the  $i$ -th component of the transformed innovation,  $\mathbf{U}^T\mathbf{R}^{-1/2}\bar{\boldsymbol{\delta}}$ , and

$$\gamma_i = \begin{cases} 1 & \text{for } \hat{\beta}_{\mathbf{R}} \\ (1 + \sigma_i^2)^{-1} & \text{for } \hat{\beta}_{\bar{\mathbf{C}}} \\ (\sigma_i^2)^{-1} & \text{for } \hat{\beta}_{\mathbf{H}\bar{\mathbf{B}}\mathbf{H}^T} \\ (1 + \sigma_i^2)/(1 + \hat{\beta}\sigma_i^2)^2 & \text{for } \hat{\beta}_{\text{ML}} \end{cases} \quad (88)$$

The condition equation (87) may be solved explicitly for  $\hat{\beta}$ , except in the case of  $\hat{\beta}_{\text{ML}}$ . Nevertheless, equations (87) and (88) may be used to provide an insight on the bias of  $\hat{\beta}_{\text{ML}}$ , a subject of study since Mitchell and Houtekamer [2000]. Indeed, note that while the full matrix,  $\bar{\mathbf{B}}$ , is an unbiased estimator of  $\mathbf{B}$ , the spectrum of  $\bar{\mathbf{B}}$  is a biased estimate of the spectrum of  $\mathbf{B}$  [Takemura, 1984; van der Vaart, 1961]. Thus the spectrum of  $\mathbf{H}\bar{\mathbf{B}}\mathbf{H}^T\mathbf{R}^{-1}$ , namely  $\{\sigma_i^2\}_{i=1, \dots, P}$ , is also biased. Hence, generally, functions of the spectrum will be biased – an important exception being that  $\mathbb{E}(\sum_i \sigma_i^2) = \text{tr}(\mathbf{H}\bar{\mathbf{B}}\mathbf{H}^T\mathbf{R}^{-1})$ . Therefore, considering the relatively complicated expression of its  $\gamma_i$ , it seems logical that the bias of  $\{\sigma_i^2\}_{i=1, \dots, P}$  will significantly carry over into  $\hat{\beta}_{\text{ML}}$ . Numerical experiments confirm this, and show that the bias of  $\hat{\beta}_{\text{ML}}$  is worse than it is for  $\hat{\beta}_{\mathbf{R}}$ , but less than for  $\hat{\beta}_{\bar{\mathbf{C}}}$  and  $\hat{\beta}_{\mathbf{H}\bar{\mathbf{B}}\mathbf{H}^T}$ .

Why is the bias of  $\hat{\beta}_{\mathbf{R}}$  of equation (44) the least? Loosely speaking, because the trace of  $\bar{\mathbf{B}}$  is taken before the division. This can be seen by studying the case where  $\mathbf{R}$  and  $\mathbf{H}\bar{\mathbf{B}}\mathbf{H}^T$  have the same structure, i.e.  $\mathbf{H}\bar{\mathbf{B}}\mathbf{H}^T\mathbf{R}^{-1} = \sigma^2\mathbf{I}_P$ , because then the bias can be obtained analytically, as follows. Assuming the ensemble is sampled from the same Gaussian (5) as the truth, except for the scaling  $\beta$ , then  $\bar{\mathbf{B}} \sim \mathcal{W}^{+1}(\mathbf{B}/\beta, N-1)$ , as per equation (14). Thus, the diagonal elements of  $\mathbf{R}^{-1/2}\mathbf{H}\bar{\mathbf{B}}\mathbf{H}^T\mathbf{R}^{-1/2}$  are iid, with

distribution  $\chi^{+2}(\sigma^2/\beta, N-1)$ . Taking the trace increases the certainty to  $\nu = P(N-1)$ . Moreover, since the trace is invariant to similarity transforms,  $\text{tr}(\mathbf{H}\mathbf{B}\mathbf{H}^T\mathbf{R}^{-1}) = \text{tr}(\mathbf{R}^{-1/2}\mathbf{H}\mathbf{B}\mathbf{H}^T\mathbf{R}^{-T/2})$ , and hence

$$\bar{\sigma}^2 \sim \chi^{+2}(\sigma^2/\beta, \nu). \quad (89)$$

Then, according to Table 2,  $\mathbb{E}[1/\bar{\sigma}^2] = \frac{\nu}{\nu-2}\beta/\sigma^2$ . Meanwhile,  $\mathbb{E}[\bar{\boldsymbol{\delta}}\bar{\boldsymbol{\delta}}^T] = \mathbf{R} + (1 + 1/\beta N)\mathbf{H}\mathbf{B}\mathbf{H}^T$  so that  $\mathbb{E}[\|\bar{\boldsymbol{\delta}}\|_{\mathbf{R}}^2/P - 1] = (1 + 1/\beta N)\sigma^2$ . Now, the sample mean and variance of Gaussian samples are independent. Hence, the nominator and denominator of  $\hat{\beta}_{\mathbf{R}}$  of equation (44) are independent, and the above expectations can be inserted directly to yield:

$$\mathbb{E}[\hat{\beta}_{\mathbf{R}}] = (1 + 1/\beta N)\frac{\nu}{\nu-2}\beta, \quad (90)$$

which is close to  $\beta$  for large  $N$  and  $P$ .

## F Forecasting hyperparameters

The forecast of the inflation distribution consists of equations (57a) and (57b). These are ad-hoc and not straightforward to derive. Similar forecast equations have been proposed in several references among the adaptive inflation literature [Anderson, 2007, 2009; Nakabayashi and Ueno, 2017; Sarkka and Hartikainen, 2013; Sarkka and Nummenmaa, 2009], under the heading of “relaxation”, “forgetting”, or “spreading”. However, it has been seen as heuristic, because it has not been derived through the Chapman-Kolmogorov equation, using a transition kernel,  $p(\beta_k|\beta_{k-1})$ , and possibly an underlying “dynamical” or “physical” model. While this issue is largely academic, the lack of formality has been perceived as a difficulty. The following discusses possible resolutions.

### F.1 Independence assumptions

A separated forecast implies particular independence assumptions; these are here developed explicitly. The Chapman-Kolmogorov forecast equation for  $(\mathbf{x}, \beta)$  reads:

$$p(\mathbf{x}_k, \beta_k) = \iint p(\mathbf{x}_k, \beta_k|\mathbf{x}_{k-1}, \beta_{k-1})p(\mathbf{x}_{k-1}, \beta_{k-1})d\beta_{k-1}d\mathbf{x}_{k-1}, \quad (91)$$

where the conditioning on  $\mathbf{y}_{k-1:1}$  is not explicitly noted.

The transition kernel factorizes as  $p(\mathbf{x}_k, \beta_k|\mathbf{x}_{k-1}, \beta_{k-1}) = p(\mathbf{x}_k|\beta_k, \mathbf{x}_{k-1}, \beta_{k-1})p(\beta_k|\mathbf{x}_{k-1}, \beta_{k-1})$ , where the cancellation follows by the removal of the red, dashed arrow in Figure 6. This removal follows from the independence of the model noise  $\boldsymbol{\xi}_k$  of equation (1a), assuming  $\beta$  is related to  $\mathbf{x}$  only through the noise. By contrast, the removal of the blue, dotted arrow constitutes an additional assumption. It yields  $p(\beta_k|\mathbf{x}_{k-1}, \beta_{k-1}) = p(\beta_k|\beta_{k-1})$  and, by the symmetry of independence,  $p(\mathbf{x}_{k-1}|\beta_k, \beta_{k-1}) = p(\mathbf{x}_{k-1}|\beta_{k-1})$ . But the previous

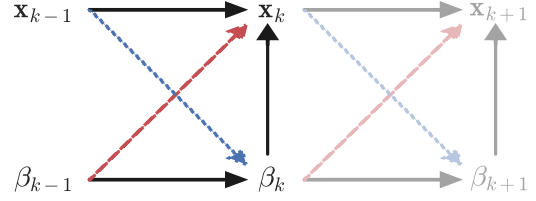


**Figure 6:** Bayesian network graph of the process  $\{\mathbf{x}_k, \beta_k\}_{k \geq 0}$ . The graph is used to represent (in)dependencies without specifying their specific functional forms. The arrows designate conditional dependencies and their causal direction.

analysis culminates a posterior that is decoupled, as discussed for equation (64); this expresses the independence  $p(\mathbf{x}_{k-1}, \beta_{k-1}) \approx p(\mathbf{x}_{k-1})p(\beta_{k-1})$  and yields  $p(\mathbf{x}_{k-1}) = p(\mathbf{x}_{k-1}|\beta_{k-1}) = p(\mathbf{x}_{k-1}|\beta_k)$ . Thus, equation (91) factorizes into:

$$p(\mathbf{x}_k, \beta_k) = p(\mathbf{x}_k|\beta_k)p(\beta_k), \quad (92)$$

where

$$p(\mathbf{x}_k|\beta_k) = \int p(\mathbf{x}_k|\beta_k, \mathbf{x}_{k-1})p(\mathbf{x}_{k-1})d\mathbf{x}_{k-1}, \quad (93a)$$

$$p(\beta_k) = \int p(\beta_k|\beta_{k-1})p(\beta_{k-1})d\beta_{k-1}. \quad (93b)$$

Note that in the forecasted prior, equation (92),  $\mathbf{x}_k$  and  $\beta_k$  are not independent. Equation (93a) is computed approximately by the ensemble forecast. The following subsection is concerned with equation (93b).

### F.2 Explicit dynamical models for $\beta$

While the specifics of equations (57a) and (57b) are engineered, its effect of “forgetting” is a well-defined objective. This is an effect that is perhaps most simply modelled with autoregressive models, which can be put into Markov form by state augmentation [Durbin and Koopman, 2012, §3.4]. The forecast step would then be simply to “pop off” the earliest element in the state vector, and shift the others down. Depending on how the past information is stored and updated in the augmented vector, different time dependences are obtained.

A more physical model is additive noise, i.e. diffusion. This works well for Gaussian distributions and noises. But if  $p(\beta)$  is assumed  $\chi^{-2}$ , then it is not clear how to maintain this through additive noise. Moreover, Gaussian noise will cause some negative (and therefore inadmissible) inflation values.

As discussed for equation (49), Brankart *et al.* [2010] suggested exponentiating  $p(\beta)$  in the forecast step, with the effect of flattening it. This trick is known as “annealing” and is used in “multiple data assimilation” [Stordal and Elsheim, 2015], where it has the effect of widening Gaussian likelihoods. It will maintain the  $\chi^{-2}$  distribution, and the mean relaxation can be controlled by also exponentiating  $\beta$  itself. However, it is not clear

how pdf exponentiation could be physically motivated or obtained via the Chapman-Kolmogorov equations.

For the purpose of Monte-Carlo simulations, a purely stochastic model could be considered: sample  $\chi^{-2}$  completely randomly, with parameters from equations (57a) and (57b). This lacks physical motivation, however, and will introduce significant sampling noise. By contrast, a fully deterministic model can be constructed with the inverse-transform method: if  $\beta_k$  is a realization of a distribution with CDF  $F^a$ , then solving  $F^f(\beta_{k+1}) = F^a(\beta_k)$  for  $\beta_{k+1}$  yields a realization from the distribution with CDF  $F^f$ . The CDFs are perhaps easier to compute for the reciprocals,  $1/\beta$ , which are  $\chi^{+2}$ . However, the approach still seems overly costly, while lacking in physical motivation. Something in between the inverse-transform method and the resampling method can be imagined, but the cost-benefit is questionable.

It could also be argued that the search for physical dynamics is misguided. After all, the inflation,  $\beta$ , is a hyperparameter. So why should it be more natural to forecast  $\beta$  rather than the hyper-hyperparameters,  $\beta^{a,f}$  and  $\nu_k^{a,f}$ ?

## Acknowledgements

The authors thank A. Farchi for technical help and discussions; L. Bertino for fostering the collaboration and for his patience; C. Grudzien for insight on the behaviour of the Lorenz system; F. Counillon, for reading and opinion; A. Karspeck and M. Gharamti for stimulating questions. Author P. N. Raanes acknowledges funding from the project EmblAUS of the Nordic Countries funding agency NordForsk. Author A. Carrassi has been partly funded by the project REDDA of the Norwegian Research Council. CEREA is thanked for providing office space and community for visiting researcher P. N. Raanes. CEREA is a member of the Institut Pierre-Simon Laplace (IPSL).

## References

- Anderson JL. 2007. An adaptive covariance inflation error correction algorithm for ensemble filters. *Tellus A* **59**(2): 210–224.
- Anderson JL. 2009. Spatially and temporally varying adaptive covariance inflation for ensemble filters. *Tellus A* **61**(1): 72–83.
- Anderson JL, Anderson SL. 1999. A Monte Carlo implementation of the nonlinear filtering problem to produce ensemble assimilations and forecasts. *Monthly Weather Review* **127**(12): 2741–2758.
- Asch M, Bocquet M, Nodet M. 2016. *Data assimilation: methods, algorithms, and applications*. Fundamentals of Algorithms, SIAM: Philadelphia, PA, doi:10.1137/1.9781611974546.
- Azevedo-Filho A, Shachter RD. 1994. Laplace’s method approximations for probabilistic inference in belief networks with continuous variables. In: *Proceedings of the Tenth international conference on Uncertainty in artificial intelligence*. Morgan Kaufmann Publishers Inc., pp. 28–36.
- Berry T, Harlim J. 2014. Linear theory for filtering nonlinear multiscale systems with model error. *Proceedings of the Royal Society A: Mathematical, Physical and Engineering Science* **470**(2167): 20140168.
- Bishop CH, Etherton BJ, Majumdar SJ. 2001. Adaptive sampling with the ensemble transform Kalman filter. Part I: Theoretical aspects. *Monthly Weather Review* **129**(3): 420–436.
- Bocquet M. 2011. Ensemble Kalman filtering without the intrinsic need for inflation. *Nonlinear Processes in Geophysics* **18**(5): 735–750.
- Bocquet M, Carrassi A. 2017. Four-dimensional ensemble variational data assimilation and the unstable subspace. *Tellus A: Dynamic Meteorology and Oceanography* **69**(1): 1304504.
- Bocquet M, Gurumoorthy KS, Apte A, Carrassi A, Grudzien C, Jones CKRT. 2017. Degenerate kalman filter error covariances and their convergence onto the unstable subspace. *SIAM/ASA Journal on Uncertainty Quantification* **5**(1): 304–333.
- Bocquet M, Raanes PN, Hannart A. 2015. Expanding the validity of the ensemble Kalman filter without the intrinsic need for inflation. *Nonlinear Processes in Geophysics* **22**(6): 645–662.
- Bocquet M, Sakov P. 2012. Combining inflation-free and iterative ensemble Kalman filters for strongly nonlinear systems. *Nonlinear Processes in Geophysics* **19**(3): 383–399.
- Bocquet M, Sakov P, *et al.* 2013. Joint state and parameter estimation with an iterative ensemble Kalman smoother. *Nonlinear Processes in Geophysics* **20**(5): 803–818.
- Brankart JM, Cosme E, Testut CE, Brasseur P, Verron J. 2010. Efficient adaptive error parameterizations for square root or ensemble Kalman filters: application to the control of ocean mesoscale signals. *Monthly Weather Review* **138**(3): 932–950.
- Chapnik B, Desroziers G, Rabier F, Talagrand O. 2006. Diagnosis and tuning of observational error in a quasi-operational data assimilation setting. *Quarterly Journal of the Royal Meteorological Society* **132**(615): 543–565.
- Daley R. 1992. Estimating model-error covariances for application to atmospheric data assimilation. *Monthly Weather Review* **120**(8): 1735–1746.

- Dee D, Cohn S, Dalcher A, Ghil M. 1985. An efficient algorithm for estimating noise covariances in distributed systems. *IEEE transactions on automatic control* **30**(11): 1057–1065.
- Dee DP. 1995. On-line estimation of error covariance parameters for atmospheric data assimilation. *Monthly Weather Review* **123**(4): 1128–1145.
- Dee DP, Da Silva AM. 1999. Maximum-likelihood estimation of forecast and observation error covariance parameters. Part I: Methodology. *Monthly Weather Review* **127**(8): 1822–1834.
- Desroziers G, Berre L, Chapnik B, Poli P. 2005. Diagnosis of observation, background and analysis-error statistics in observation space. *Quarterly Journal of the Royal Meteorological Society* **131**(613): 3385–3396.
- Desroziers G, Ivanov S. 2001. Diagnosis and adaptive tuning of observation-error parameters in a variational assimilation. *Quarterly Journal of the Royal Meteorological Society* **127**(574): 1433–1452.
- Dreano D, Tandeo P, Pulido M, Ait-El-Fquih B, Chonavel T, Hoteit I. 2017. Estimating model-error covariances in nonlinear state-space models using kalman smoothing and the expectation-maximization algorithm. *Quarterly Journal of the Royal Meteorological Society* **143**(705): 1877–1885.
- Durbin J, Koopman SJ. 2012. *Time series analysis by state space methods*, vol. 38. OUP Oxford.
- Einicke GA. 2012. *Nonlinear prediction, filtering and smoothing, smoothing, filtering and prediction - estimating the past, present and future*. InTech, doi: 10.5772/39258.
- Evensen G. 2009a. *Data assimilation*. Springer, 2 edn.
- Evensen G. 2009b. The ensemble Kalman filter for combined state and parameter estimation. *Control Systems, IEEE* **29**(3): 83–104.
- Fernandez C, Steel MFJ. 1999. Multivariate Student-t regression models: Pitfalls and inference. *Biometrika* **86**(1): 153–167.
- Fitzgerald R. 1971. Divergence of the Kalman filter. *Automatic Control, IEEE Transactions on* **16**(6): 736–747.
- Frei M, Künsch HR. 2012. Sequential state and observation noise covariance estimation using combined ensemble Kalman and particle filters. *Monthly Weather Review* **140**(5): 1476–1495.
- Furrer R, Bengtsson T. 2007. Estimation of high-dimensional prior and posterior covariance matrices in Kalman filter variants. *Journal of Multivariate Analysis* **98**(2): 227–255.
- Gelman A, Carlin JB, Stern HS, Rubin DB. 2004. *Bayesian data analysis*. Texts in Statistical Science Series, Chapman & Hall/CRC, Boca Raton, FL, second edn.
- Geweke J. 1993. Bayesian treatment of the independent student-t linear model. *Journal of applied econometrics* **8**(S1).
- Gharanti ME. 2017. Enhanced adaptive inflation algorithm for ensemble filters. *Monthly Weather Review* **In review**(0): 0–0.
- Goutis C, Casella G. 1999. Explaining the saddlepoint approximation. *The American Statistician* **53**(3): 216–224.
- Grudzien C, Carrassi A, Bocquet M. 2017. Chaotic dynamics and the role of covariance inflation for reduced rank kalman filters with model error. *Nonlinear Processes in Geophysics* .
- Hamill TM, Whitaker JS, Snyder C. 2001. Distance-dependent filtering of background error covariance estimates in an ensemble Kalman filter. *Monthly Weather Review* **129**(11): 2776–2790.
- Haussaire JM. 2017. Thesis. PhD thesis, CERE. TODO.
- Hunt BR, Kalnay E, Kostelich EJ, Ott E, Patil DJ, Sauer T, Szunyogh I, Yorke JA, Zimin AV. 2004. Four-dimensional ensemble Kalman filtering. *Tellus A* **56**(4): 273–277.
- Hunt BR, Kostelich EJ, Szunyogh I. 2007. Efficient data assimilation for spatiotemporal chaos: A local ensemble transform Kalman filter. *Physica D: Nonlinear Phenomena* **230**(1): 112–126.
- Jaynes ET. 2003. *Probability theory: the logic of science*. Cambridge university press.
- Kotsuki S, Ota Y, Miyoshi T. 2017. Adaptive covariance relaxation methods for ensemble data assimilation: Experiments in the real atmosphere. *Quarterly Journal of the Royal Meteorological Society* .
- Le Gland F, Monbet V, Tran VD. 2009. Large sample asymptotics for the ensemble Kalman filter. Research Report RR-7014, INRIA.
- Li H, Kalnay E, Miyoshi T. 2009. Simultaneous estimation of covariance inflation and observation errors within an ensemble Kalman filter. *Quarterly Journal of the Royal Meteorological Society* **135**(639): 523–533.
- Liang X, Zheng X, Zhang S, Wu G, Dai Y, Li Y. 2012. Maximum likelihood estimation of inflation factors on error covariance matrices for ensemble Kalman filter assimilation. *Quarterly Journal of the Royal Meteorological Society* **138**(662): 263–273.
- Lorenz EN. 1963. Deterministic nonperiodic flow. *Journal of the Atmospheric Sciences* **20**(2): 130–141.

- Lorenz EN. 1996. Predictability: A problem partly solved. In: *Proc. ECMWF Seminar on Predictability*, vol. 1. Reading, UK, pp. 1–18.
- Lorenz EN. 2005. Designing chaotic models. *Journal of the Atmospheric Sciences* **62**(5): 1574–1587.
- Mandel J, Cobb L, Beezley JD. 2011. On the convergence of the ensemble Kalman filter. *Applications of Mathematics* **56**(6): 533–541.
- Mehra R. 1972. Approaches to adaptive filtering. *IEEE Transactions on automatic control* **17**(5): 693–698.
- Ménard R. 2016. Error covariance estimation methods based on analysis residuals: theoretical foundation and convergence properties derived from simplified observation networks. *Quarterly Journal of the Royal Meteorological Society* **142**(694): 257–273.
- Ménard R, Cohn SE, Chang LP, Lyster PM. 2000. Assimilation of stratospheric chemical tracer observations using a Kalman filter. Part I: Formulation. *Monthly Weather Review* **128**: 2654–2671.
- Mitchell HL, Houtekamer PL. 2000. An adaptive ensemble Kalman filter. *Monthly Weather Review* **128**(2): 416–433.
- Mitchell L, Carrassi A. 2015. Accounting for model error due to unresolved scales within ensemble Kalman filtering. *Quarterly Journal of the Royal Meteorological Society* **141**(689): 1417–1428.
- Miyoshi T. 2011. The Gaussian approach to adaptive covariance inflation and its implementation with the local ensemble transform Kalman filter. *Monthly Weather Review* **139**(5): 1519–1535.
- Miyoshi T, Kalnay E, Li H. 2013. Estimating and including observation-error correlations in data assimilation. *Inverse Problems in Science and Engineering* **21**(3): 387–398.
- Mohamed AH, Schwarz KP. 1999. Adaptive Kalman filtering for INS/GPS. *Journal of geodesy* **73**(4): 193–203.
- Muirhead RJ. 1982. *Aspects of multivariate statistical theory*. John Wiley & Sons, Inc., New York. Wiley Series in Probability and Mathematical Statistics.
- Myrseth I, Omre H, *et al.* 2010. Hierarchical ensemble Kalman filter. *SPE Journal* **15**(02): 569–580.
- Nakabayashi A, Ueno G. 2017. An extension of the ensemble Kalman filter for estimating the observation error covariance matrix based on the variational Bayes’s method. *Monthly Weather Review* **145**(1): 199–213.
- Özkan E, Šmídl V, Saha S, Lundquist C, Gustafsson F. 2013. Marginalized adaptive particle filtering for nonlinear models with unknown time-varying noise parameters. *Automatica* **49**(6): 1566–1575.
- Pham DT, Verron J, Roubaud MC. 1998. A singular evolutive extended Kalman filter for data assimilation in oceanography. *Journal of Marine systems* **16**(3): 323–340.
- Raanes PN. 2016. Improvements to ensemble methods for data assimilation in the geosciences. PhD thesis, University of Oxford. <https://ora.ox.ac.uk/objects/uuid:9f9961f0-6906-4147-a8a9-ca9f2d0e4a12>.
- Raanes PN, Carrassi A, Bertino L. 2015. Extending the square root method to account for model noise in the ensemble Kalman filter. *Monthly Weather Review* **143**(10): 3857–3873.
- Roberts GO, Rosenthal JS. 2001. Infinite hierarchies and prior distributions. *Bernoulli* : 453–471.
- Roth M, Ardeshiri T, Özkan E, Gustafsson F. 2017. Robust Bayesian Filtering and Smoothing Using Student’s t Distribution. *ArXiv e-prints* .
- Sacher W, Bartello P. 2008. Sampling errors in ensemble Kalman filtering. Part I: Theory. *Monthly Weather Review* **136**(8): 3035–3049.
- Sarkka S, Hartikainen J. 2013. Non-linear noise adaptive Kalman filtering via variational Bayes. In: *Machine Learning for Signal Processing (MLSP), 2013 IEEE International Workshop on*. IEEE, pp. 1–6.
- Sarkka S, Nummenmaa A. 2009. Recursive noise adaptive Kalman filtering by variational Bayesian approximations. *IEEE Transactions on Automatic Control* **54**(3): 596–600.
- Snyder C. 2012. *Introduction to the kalman filter*, ch. 3. Advanced Data Assimilation for Geosciences: Lecture Notes of the Les Houches School of Physics: Special Issue, Oxford University Press, pp. 75–120.
- Stordal AS, Elsheikh AH. 2015. Iterative ensemble smoothers in the annealed importance sampling framework. *Advances in Water Resources* **86**: 231–239.
- Storvik G. 2002. Particle filters for state-space models with the presence of unknown static parameters. *IEEE Transactions on signal Processing* **50**(2): 281–289.
- Stroud JR, Bengtsson T. 2007. Sequential state and variance estimation within the ensemble Kalman filter. *Monthly Weather Review* **135**(9): 3194–3208.
- Stroud JR, Katzfuss M, Wikle CK. 2016. A Bayesian adaptive ensemble Kalman filter for sequential state and parameter estimation. *arXiv preprint arXiv:1611.03835* .
- Takemura A. 1984. An orthogonally invariant minimax estimator of the covariance matrix of a multivariate normal population. *Tsukuba journal of mathematics* **8**(2): 367–376.



- Tsyrlunikov M, Rakitko A. 2015. Hierarchical Bayes ensemble Kalman filtering. *Physica D: Nonlinear Phenomena* .
- Ueno G, Higuchi T, Kagimoto T, Hirose N. 2010. Maximum likelihood estimation of error covariances in ensemble-based filters and its application to a coupled atmosphere–ocean model. *Quarterly Journal of the Royal Meteorological Society* **136**(650): 1316–1343.
- Ueno G, Nakamura N. 2016. Bayesian estimation of the observation-error covariance matrix in ensemble-based filters. *Quarterly Journal of the Royal Meteorological Society* **142**(698): 2055–2080.
- van der Vaart HR. 1961. On certain characteristics of the distribution of the latent roots of a symmetric random matrix under general conditions. *The Annals of Mathematical Statistics* : 864–873.
- van Leeuwen PJ. 1999. Comment on “Data assimilation using an ensemble Kalman filter technique”. *Monthly Weather Review* **127**(6): 1374–1377.
- Wang X, Bishop CH. 2003. A comparison of breeding and ensemble transform Kalman filter ensemble forecast schemes. *Journal of the Atmospheric Sciences* **60**(9): 1140–1158.
- Whitaker JS, Hamill TM. 2012. Evaluating methods to account for system errors in ensemble data assimilation. *Monthly Weather Review* **140**(9): 3078–3089.
- Wilks DS. 2005. Effects of stochastic parametrizations in the Lorenz’96 system. *Quarterly Journal of the Royal Meteorological Society* **131**(606): 389–407.
- Wilks DS. 2011. *Statistical methods in the atmospheric sciences*, vol. 100. Academic Press.
- Wu L, Bocquet M, Chevallier F, Lauvaux T, Davis K. 2013. Hyperparameter estimation for uncertainty quantification in mesoscale carbon dioxide inversions. *Tellus B: Chemical and Physical Meteorology* **65**(1): 20894, doi:10.3402/tellusb.v65i0.20894.
- Ying Y, Zhang F. 2015. An adaptive covariance relaxation method for ensemble data assimilation. *Quarterly Journal of the Royal Meteorological Society* **141**(692): 2898–2906.
- Zheng X. 2009. An adaptive estimation of forecast error covariance parameters for Kalman filtering data assimilation. *Advances in Atmospheric Sciences* **26**(1): 154–160.